Genuense Athenaeum

Università degli Studi di Genova

Scuola Politecnica & Facoltà di Ingegneria

---

www.itim.unige.it/strategos

Laurea Magistrale in Ingegneria Strategica

International MSc in Engineering Technology for Strategy & Security of Genoa University

---

Water Polo Players Localization Using Ultra-Wide Band Technology

---

Advisors: **Prof.Ing, Agostino G. Bruzzone, Prof. Elizabeth Colin, Researcher-Teacher. Laurie Conteville**

Candidate : **Mr. Farshad Shamlu**

Academic Year 2022-2023

STRATEGOS 3rd Edition

Acknowledgements

I am deeply grateful to my advisor, Professor Agostino Bruzzone, for their exceptional guidance and unwavering support throughout my master's program. Their expertise, mentorship, and encouragement have been invaluable in shaping my research and facilitating the completion of this thesis.

I would also like to extend my heartfelt appreciation to Professor Elizabeth Colin and Teacher Laurie Conteville for their supervision and valuable feedback during my internship. Their guidance and insights have greatly enriched my learning experience, and I am grateful for the opportunity to conduct my internship at the esteemed Efrei Paris Engineering School Research Lab.

Finally, I would like to express my sincere thanks to my friends and family for their unwavering love, encouragement, and support throughout this challenging yet rewarding journey. Their presence and belief in my abilities have been a constant source of inspiration and motivation.

Abstract

This Thesis will be carried out in collaboration with the French Swimming Federation and will generally aim to provide assistance in the assessment of physical and tactical needs in water polo. To know individually the training load and the performances during a match, several indicators (the distance covered, the number of sprints, the number of dives, the maximum speed, average, etc.,) must go up to the coach. The objective of this project will be to precisely locate (about 20cm) water polo players during matches and training. For this, it will be necessary to deploy a localization system and integrate it into a swimming cap (waterproof device). Main objectives can define as Performance Optimization, Injury Prevention, Life Balance Improvement, and Training Efficiency. The initial focus lies on selecting and validating the localization technology, with Ultra-Wideband (UWB) being the preferred choice. This technology, known for its wide frequency spectrum, holds great potential for precise and accurate localization. The subsequent step involves handling the devices effectively, ensuring seamless integration into the project framework. Once the devices are in place, the deployment of a robust localization system takes center stage, setting the foundation for accurate positioning. The project team then dedicates efforts to optimize both static and moving accuracy, fine-tuning the system to deliver precise location data in various scenarios. comprehensive performance testing and evaluation are conducted, meticulously exploring the system's capabilities, and validating its effectiveness. Throughout the project, rigorous experiments were designed and carried out to assess the performance of UWB technology in accurately determining the positions of individuals within indoor sporting environments. These experiments encompassed diverse scenarios, taking into account factors such variations in movement patterns, and the presence of potential obstacles or interference. The results obtained from these experiments provide valuable insights into the effectiveness and applicability of UWB technology for indoor localization in the specific sport case study. They contribute to the body of knowledge surrounding indoor positioning systems, offering evidence to support the validation of UWB technology as a reliable solution for accurately tracking and localizing athletes or participants in indoor sporting environments.

Contents

Content of figures

INTRODUCTION

In today's era of automation and digitalization, accurate navigation of both individuals and devices within indoor environments has become crucial for a growing number of applications. While the performance of outdoor positioning has significantly improved with the emergence of global satellite positioning systems, many mass-market applications require seamless positioning capabilities in all environments. Consequently, indoor positioning has become an increasingly important focus of research and development efforts over the past decade. Indoor positioning systems aim to provide accurate and reliable location information within complex indoor environments, such as shopping malls, airports, and hospitals, where traditional GPS technology may not be sufficient. Such systems have applications in diverse fields, including athlete tracking in sport, asset tracking, logistics, emergency response, etc. The development of robust and accurate indoor positioning systems is, therefore, a critical area of research for the advancement of various industries and the improvement of daily life. Recent advancements in indoor positioning technology have led to the development of high-precision positioning systems, such as Ultra-Wideband (UWB) technology, which offers sub-meter accuracy and low latency in indoor environments.

Sciences2024 is a collaborative research program dedicated to supporting French athletes in their quest for success at the Paris 2024 Olympic and Paralympic Games. The program brings together various scientific disciplines and experts to optimize athletic performance and maximize athletes' potential. Sciences2024 aims to leverage scientific advancements and research to enhance training methodologies and improve athletes' overall performance. The program utilizes state-of-the-art technology, such as motion capture systems and wearable sensors, to gather precise data on athletes' movements, energy expenditure, and physiological responses. This data-driven approach allows for tailored training programs and interventions. Collaboration between academia, research institutions, sports federations, and athletes are a key aspect of Sciences2024. By fostering knowledge exchange and expertise, the program promotes innovation and advances the scientific understanding of sports performance.

CHAPTHER 1: Water Polo Rules and Gameplay Analysis

This section provides a comprehensive overview of the rules and gameplay of water polo, a highly competitive and physically demanding sport played in water, and to equip readers with a solid understanding of the fundamental aspects of water polo, including the rules governing the game, player positions, scoring, and essential knowledge required to excel in this sport.

History:

The captivating history of water polo traces its origins back to the Victorian English Society, emerging as a product of the industrial revolution and the burgeoning interest in sports. In the mid-1870s, as England experienced rapid urbanization due to industrialization, the construction of public baths provided the opportunity for people to both cleanse themselves and learn to swim. It was during this time that a new aquatic game, dubbed "football in the water," began to take shape.

Between 1877 and 1885, English Clubs introduced the game within swimming clubs, and the English Swimming Association established the first set of rules. Concurrently, water polo was already being played in Scotland. The inaugural national championships were held in 1886 in Scotland and 1888 in England. Initially, water polo was an exclusively male competition, characterized by raw strength and swimming prowess. From 1890 to 1900, water polo rapidly gained popularity across Europe, leading to the organization of numerous tournaments in countries such as Germany, Austria, France, Belgium, Hungary, and Italy. These competitions followed the rules developed in England. The significance of water polo expanded further when it made its Olympic debut at the 1900 Games in Paris, marking the second edition of the Olympics. The participating teams represented their respective countries, showcasing the global reach of the sport.

A significant milestone in the evolution of water polo occurred in 1908 with the establishment of FINA (Fédération Internationale de Natation), which standardized the rules and regulations governing the sport. By 1911, countries around the world were playing water polo based on the same set of rules. During this period, Great Britain emerged as a dominant force in international water polo.Despite the setbacks caused by the First World War, the popularity of water polo continued to spread globally. The sport persisted and thrived, captivating athletes and enthusiasts alike, shaping the competitive landscape of aquatic sports.

Figure 1: England 1900, an early water polo game

The rich history of water polo stands as a testament to its enduring appeal and remarkable journey from its humble beginnings to becoming an established and respected sport worldwide. It serves as a reminder of the sport's evolution, its ability to transcend borders, and the passion and dedication of those who have contributed to its growth and success.[61]

Rules and Regulations:

The Field of play: The overall Field of Play will be 30.60m * 20.00m for men and 25.60m * 20.00m for women. The distance between the goal lines shall not be less than 20 meters and not more than 30 meters for games played by men. The distance between the goal lines shall not be less than 20 meters and not more than 25 meters for games played by women. The width of the field of play shall be not less than 10 meters and not more than 20 meters.

Official table: The designated location where other necessary officials and authorized persons carry out their responsibilities during a game.

Flying Substitution Area: The area designated by the Rules at the side of the Field of Play where flying substitutions may occur (Red Area on Figure 1.2).

Goal line: the end of the field of play, formed by the front face of the goal post.

Goal area: Is a rectangular box extending 2 meters from the lateral outsides of the goal posts to the 2-meter line opposite the goal line. In this area, attacking players must not enter without possession of the ball, unless they are behind the line of the ball.

5-meter line: Is the line from where penalty throw should be taken.

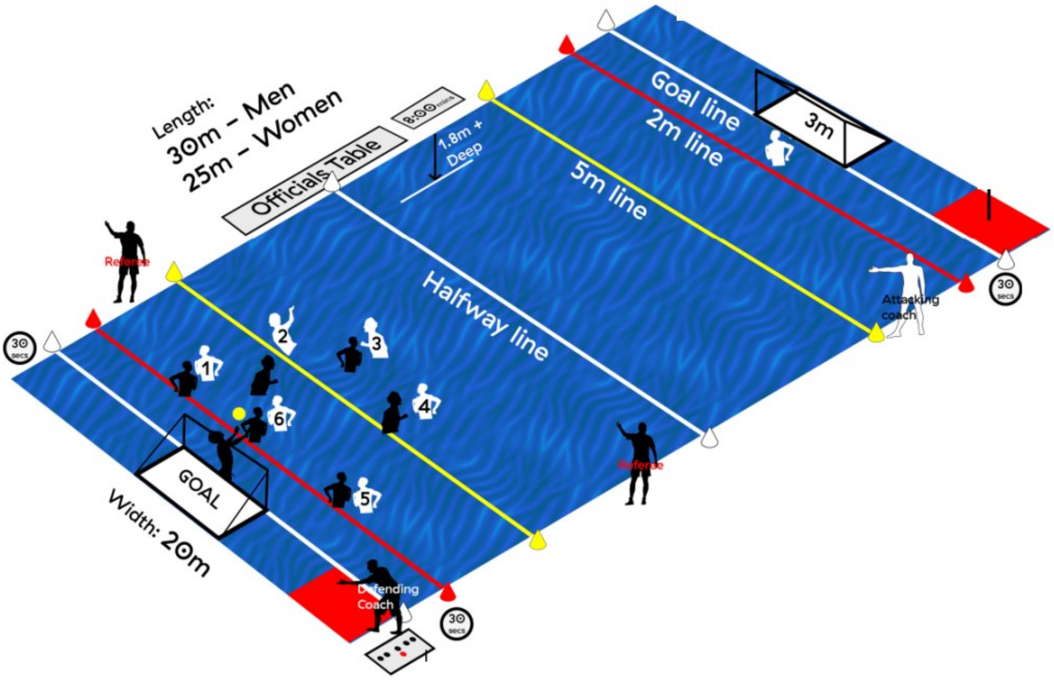

Figure 3: Water polo FINA rules and regulations

6-meter area: is an area within 6 meters of the goal line where some fouls according to the penalty rules, become a penalty foul.

Half distance line: Line which divides the length of the field of play into two equal halves at its midpoint.

Goalkeeper: individual member of a team, wearing a cap 1 or 13, whose main role is to prevent the ball from entering the goal.

Advantage: The opportunity of an attacking player and/ or the attacking team to continue to play the ball to generate an opportunity to score. Referees must officiate such that the attacking team can maintain its advantage.

Red Card: Signal from the referee to indicate an exclusion from the remainder of the game to a player, coach, or any team official.

Yellow Card: Warning signal from the referee to the coach for inappropriate behavior or insufficient bench discipline, or for repeated simulation and persistent foul play of a team.

Referee: An official responsible for conducting the game with designated functions fixed by the Rules.

Possession Clocks: Teams have 30 seconds to shoot, and Time resets on shots and exclusions.

Start of Periods: All players line up behind the goal line, referee whistles and players sprint for ball on halfway line.

Scoring: Ball must be 100% over goal line to score and can score with any part of body except clenched fist.

Players: Each team must consist of a maximum of thirteen players: eleven field players and two goalkeepers. A team must start the game with not more than seven players, one of whom shall be the goalkeeper and who shall wear the goalkeeper's cap. Five reserves may be used as substitutes and one reserve goalkeeper who may be used only as a substitute goalkeeper. A team playing with less than seven players shall not be required to have a goalkeeper. If a team has no more substitutes apart from the substitute goalkeeper, either the goalkeeper or substitute goalkeeper, if applicable, may play as a field player.

Substitutes: At any time in the game, a player or goalkeeper may be substituted by leaving the field of play at the team's exclusion re-entry area. The substitute may enter the field of play from the exclusion re-entry area as soon as the player has visibly risen to the surface of the water within the re-entry area and touched hands above the water with the substitute. Substitution from the 'flying substitution' area is also allowed when the substitute enters the area from behind the extended goal line, both players, the exiting player and the substitute, are in the water, outside of the field of play and touch hands above the water. A substitute shall be ready to replace a player, without delay. If the substitute is not ready, the game shall continue without the substitute and, at any time, the substitute may then enter the field of play from the team's designated substitution areas, after touching hands where applicable.

Referees: For World Aquatics events, the officials shall consist of two referees, two assistant referees, timekeepers and secretaries and a video assistant referee, each with the powers and duties specified in.

Game duration: Teams play four periods, each period consisting of eight minutes of actual playing time; a total of 32 minutes. Actual play starts at the beginning of each period, when a player touches the ball, stops on every stoppage indicated by the referee or shot clock and continues after every stoppage when the player puts the ball into play according to the Rules, shoots or passes the ball. The quarter breaks are 2 minutes, and half time is 5 minutes long.

Timeout: A one-minute stoppage of play available to the attacking team at any time, except at the awarding of a penalty throw or during a VAR review. Each team is entitled to two timeouts per game. Each timeout is 1 minute.

Ordinary fouls:

False Start: To begin the start of play improperly, either before the signal from the referee or pushing off from or affecting the alignment of the goal.

Foul: A violation of a rule resulting in a stoppage of the game clock and the awarding of a free throw. There are two types of fouls:

- Physical fouls (physical contact of a player preventing an opposing player from continuing with movement)
- Technical fouls (against rules, e.g., false start or restart, to strike the ball with clenched fist, two hands, etc.)

Ball under: Ordinary foul called against a player for taking the ball under water when tackled by an opponent or with intent to hide a ball from an opponent.

Push-off: To use the hand, arm, foot, or another body part to push off an opponent to gain an advantage.

Kicking: A blow, strike or forceful thrust with the foot to an opponent's body or face, which is a personal foul.

Simulation: To pretend to be fouled.

To drive: An attacking move by a player who is facing an opponent and who attempts to aggressively swim by that player to a position of advantage closer to the goal.

To tackle: To hold, sink, pull back or impede a player who is holding the ball.

Holding the ball: Lifting, carrying or touching the ball but not including dribbling the ball.

Exclusion fouls:

Improper Entry: Entry of a player into the game during play not in accordance with the rules.

Exclusion Foul: A foul where a player is excluded from taking part in the game for a period as prescribed in the Rules.

Misconduct: Any improper behavior, including being disrespectful towards a referee or opponent, as well as showing disregard for an instruction from the referee.

Violent action: An action by a player intended to cause harm or to injure another player or official, regardless of whether contact is made.

Aggressive foul play: Behavior that can lead to injuries of opponents. The intention of these kinds of fouls is to destroy and completely stop the advantage or progress of the game or a player, or to provoke the opponent.

To Impede: To obstruct movement with unallowed physical acts, like holding or blocking an opponent.

To hold an opponent: To use the hands, arms or legs to hold onto an opponent with the intention of restricting movement.

To sink: To push an opponent under the water.

To Pull back: To pull an opposing player.

To interfere with a free throw, goal, or penalty throw: To disrupt or interfere with the taking of any of these throws.

Disproportionate movements: To make any movement with intent to kick or strike, even if the player fails to make contact.

Counterattack: The transition by the attacking team that brings the ball quickly from one end of the field to the other in an attempt to score before the defensive team can get into position.

CHAPTHER 2: Ultra-Wide Band Technology

Indoor Positioning Systems (IPSs) leverage a diverse range of signal technologies, including radio frequency, infrared, ultrasonic, inertial, optical, and electromagnetic. These technologies work collectively to estimate the location of the target device within indoor spaces. To achieve accurate positioning results, IPSs often combine measurements from two or more signal technologies. However, different indoor positioning applications may have varying performance requirements. Therefore, the selection of the appropriate technology becomes crucial in meeting these specific application needs.

Ultra-Wideband (UWB) is a wireless short-range radio technology that utilizes a wide spectrum to propagate information. This is achieved through the modulation of either a carrier-based waveform or a carrier-less baseband signal in the form of short-width pulses. As defined by the Federal Communication Commission (FCC) and the International Telecommunication Union (ITU)-R, UWB is characterized by a spectrum occupying a bandwidth greater than 20% of the central frequency or having a bandwidth of at least 500 MHz. The UWB RF signal operates within an ultra 500 MHz bandwidth, enabling the transmission of large data sizes while consuming lesser energy compared to other technologies. In distinguishing between narrowband (NB), wideband (WB), and UWB, the FCC classification scheme utilizes a dimensionless, frequency-independent indicator known as fractional bandwidth (BF).

In 2002, the Federal Communication Commission (FCC) recognized UWB technology as a promising and emerging advancement with wide-ranging applications. These applications include imaging systems, ground-penetrating radars (GPRs), wall-imaging systems, medical systems, surveillance systems, vehicular radar systems, communications, and measurement systems. UWB technology possesses the capability to transmit high data rates using tiny pulses spread over wider frequency bands, resulting in a low power spectral density (PSD). This characteristic enables UWB signals to exhibit exceptional penetration capability compared to most RF waves. Additionally, certain UWB signal types, like impulse radio UWB, do not require sinusoidal carrier waves, further reducing the power required for transmission.

Given these advantages, UWB emerges as a prominent candidate for real-time applications, including tracking and navigation, sensor network communications, ranging and imaging, and extremely high-data-rate short-range communication (e.g., wireless UWB). The adoption of UWB has gained momentum in personal area networks (PANs), precise indoor positioning, and indoor tracking and navigation systems. UWB positioning relies on the unique radio frequency characteristics associated with UWB technology to provide accurate indoor location estimates based on time of arrival (TOA), angle of arrival (AOA), and time difference of arrival (TDOA) of the signal. The UWB positioning signal is characterized by a low-power, short-pulse transmission with a large bandwidth which imparts robustness, precision, and security to the system.

ADVANTAGES:

In 2002, the Federal Communication Commission (FCC) granted public access to UWB technology, which was previously exclusively used for classified applications by the US military. UWB signals are characterized by short pulses transmitted over large bandwidth ranges, typically between 3.1 and 10.6 GHz, giving UWB a clear advantage over narrowband (NB) signals. The significant bandwidth and short duty cycle of UWB result in a higher data rate and capacity, making it a suitable choice for implementing RF-based Indoor Positioning Systems (IPS).

One of the key advantages of UWB is that it operates in the unlicensed spectrum, allowing anyone to use it without prior notification. Additionally, the pulse nature of the UWB signal enhances its penetration capability, enabling UWB tags on mobile targets to function without requiring a direct line of sight (LOS) with their anchors. However, in dense environments, certain scenarios may negatively affect UWB signals, leading to issues such as multipath deterioration and interference with neighboring frequencies in the spectrum. Moreover, due to the low transmission power of UWB, it may be less effective in large indoor spaces, as the signal cannot travel over long distances due to path loss attenuation. Consequently, the use of additional UWB anchors becomes necessary to ensure adequate coverage, which in turn increases costs and complexity. Despite these challenges, UWB remains a compelling choice for IPS implementation, particularly in scenarios where high data rates, precise positioning, and non-line-of-sight capabilities are crucial.

UWB technology brings forth a multitude of advantages over narrowband signals, significantly expanding its potential applications. One of the primary benefits is that UWB operates in an unlicensed and free spectrum, enabling its use without the need for prior licensing. Before its commercial availability in 2002, the UWB spectrum was restricted to military operators, particularly the Department of Defense, for classified applications. UWB's superiority stems from its significantly larger bandwidth, spanning from 3.1 to 10.6 GHz. This expansive bandwidth empowers UWB with enhanced capabilities in various aspects, making it a compelling choice for diverse positioning techniques and applications. UWB communication systems exhibit remarkable robustness and performance owing to their large bandwidth. With data rates of up to 110 Mbps, UWB surpasses other RF technologies, establishing itself as a leader in precise positioning capabilities. The significant bandwidth also allows UWB systems to operate effectively in low signal-to-noise-ratio (SNR) communication channels, offering immunity against multipath degradation. The pulse-based nature of UWB RF communication contributes to its exceptional multipath resolution. Each pulse occupies the entire bandwidth, setting it apart from carrier-based communications. As a result, UWB systems can function without requiring a clear line of sight (LOS) and are perfectly capable of operating under non-line-of-sight (NLOS) conditions. However, in positioning applications, NLOS scenarios may lead to erroneous sensor readings, potentially impacting position estimation.

Furthermore, the short-pulse, low-power nature of UWB signals presents a significant advantage for indoor positioning applications. UWB transmits at low average power due to the short-pulse nature, which submerges the signal within the noise floor (-40 dBm/MHz). This feature not only conserves transmitter energy and enhances battery life but also grants resistance against jamming and interception. These combined attributes make UWB an excellent choice for various indoor positioning and communication needs.

CHALLENGES:

While UWB technology offers numerous advantages for indoor positioning applications, it also faces challenges and drawbacks that can impact its performance. Despite being known for its coexistence with other RF systems, UWB can still cause interference to existing nearby RF systems and vice versa, leading to potential issues with GPS, 3G, and WiMAX communication systems. To address this, many countries have imposed regulations to mitigate interference. The low-power transmission of UWB is considered advantageous, but it also limits the overall power consumption for both the transmitter and receiver. This limitation can restrict the range of UWB anchors and necessitate the use of more anchors to compensate, resulting in reduced scalability and increased system complexity and computational load. Additionally, processing wide-band signals can lead to high power consumption, but a multiband approach splitting the signal into sub-bands can help mitigate this. The short pulse nature of UWB signals presents another challenge as it requires longer synchronization times, limiting data capacity and increasing the number of multipath components. Researchers have proposed solutions, such as special schemes and protocols to avoid repeated synchronization, and the use of multiple-input multiple-output systems to mitigate the effects of short communications. Lastly, UWB's usage outdoors is limited due to regulations in various countries, where fixed UWB transmitters are not allowed. These challenges highlight the need for careful consideration and innovative approaches when implementing UWB technology in indoor positioning systems.

MDEK1001 kit:

Qorvo's MDEK1001 ultra-wide band (UWB) development kit provides customers with the necessary hardware, software, and development environment to quickly evaluate Qorvo's UWB technology for use in a scalable real time location system (RTLS). This kit includes 12 DWM1001-DEV development boards in plastic enclosures. Each can be configured as an anchor, tag, or bridge node. Qorvo's DWM1001-DEV is a plug-and-play development board for evaluating the features and performance of the DWM1001C ultra-wide band (UWB) transceiver module. Users of this development board can easily assemble a fully wireless real time location system (including anchors, tags & gateways) without designing any hardware or writing a single line of code and quickly progress into developing an application. Qorvo's DWM1001 module is based on the DW1000 ultra-wideband (UWB) transceiver IC, which is an IEEE 802.15.4a UWB implementation. It integrates UWB (Ch.5) and Bluetooth antenna, all RF circuitry, Nordic Semiconductor nRF52832 and a motion sensor. Qorvo's DW1000 is a fully integrated single chip ultra-wideband (UWB) low-power, low-cost transceiver IC compliant to IEEE 802.15.4a. It can be used in 2-way ranging or TDoA location systems to locate assets to a precision of 10 cm. It also supports data transfer at rates up to 6.8 Mbps.

This MDEK1001 evaluation kit based on Decawave’s DW1000 IC & DWM1001 module is intended solely for use by competent engineering personnel for the purposes of evaluating the use of Decawave’s DW1000 IC & DWM1001 module in wireless location and communications systems. The module may be configured to behave as an “anchor” one of the fixed nodes in the system or a “tag” one of the mobile located nodes in the system. The module configuration may be achieved via Bluetooth using the companion application (Decawave DRTLS Manager). The module incorporates Decawave’s DW1000 UWB transceiver which the module’s onboard firmware drives to implement the network of anchor nodes and perform the two-way ranging exchanges with the tag nodes enabling each tag to compute its own location.

Figure 3: MDWK1001 Ultra-Wideband (UWB) Transceiver Development Kit

The module development board has a voltage supply requirement of 3.6V to 5.5V

The DWM1001 module is based on Decawave's DW1000 Ultra-Wideband (UWB) transceiver IC, which is an IEEE 802.15.4-2011 UWB implementation. It integrates UWB and Bluetooth antenna, all RF circuitry, Nordic Semiconductor nRF52832 and motion sensor.

The effect of channel characteristics on time-stamp accuracy in DW1000 based systems

When considering a channel between a transmitter and a receiver in a radio scheme one of the most important properties of the channel is whether it is either:

1. Line of Sight (LOS); or
2. Non-Line of Sight (NLOS)

The channel can have many other properties but for the purposes of this note we will concern ourselves with this primary distinction.

In this note it is important to understand the distinction between the following terms:

Communications range: The range between two DW1000 nodes at which successful communications takes place (as defined by acceptable packet error rate for a given application). The total energy transmitted into the channel by the transmitter and received at the receiver over all paths between the two nodes. If this is above the receiver sensitivity, then communications can occur.

Direct path detection range: The range between two DW1000 nodes at which the DW1000 can correctly detect and timestamp the direct path signal between the two nodes rather than any multipath. The energy received at the receiver only over the direct path between the transmitter and receiver. This energy must be above a dynamically adjusted threshold in order for it to be detected by the DW1000.

The DW1000 operates by deriving the impulse response of the communications channel between the transmitter and receiver for each received frame. It does this by processing the preamble sequence which comes at the start of every IEEE802.15.4-2011 UWB frame.

his allows the IC to:

- Detect the signal from below the noise floor
- Extract the direct path signal and any multipath signals that follow it.
- Process the impulse response and timestamp the first peak in this response that exceeds a dynamically adjusted detection threshold.

It is important to make the distinction between an optically clear line of sight and clear line of sight from an RF perspective:

- An optically clear LOS exists when no physical objects obstruct viewing one antenna from the location of the other antenna.
- An RF clear line of sight exists if a defined area around the optical line of sight, known as the Fresnel Zone, is clear of obstacles.
- For communications between DW1000 devices, it is the RF line of sight that is of interest.

to maximize range:

- Transmit power needs to be kept at the maximum allowable limit to ensure the maximum energy is transmitted into the channel. These limits are set by regulatory bodies in different parts of the world and for normal UWB operation this is usually -41.3 dBm / MHz.
- Losses due to PCB and antenna effects need to be kept to a minimum (in the case of the antennas in the DecaWave EVK1000 they should be mounted tightly to the EVB1000 boards to prevent impedance mismatch and leakage). It is important that PCB layout guidelines are followed and impedances are correctly matched.
- The lowest channel frequency possible should be used if maximum range is the overriding requirement. Receiver sensitivity is quoted in the DW1000 datasheet and depends on a number of parameters including the selected channel and the data rate. For longest range the lowest data rate (110 kbps) should be used.

CHAPTHER 3: Experimental Setup:

The experiments were conducted by using MDEK1001 kit and implementing an Ultra-Wideband (UWB) Real-Time Location System (RTLS) involves several steps to set up the system. Here's an overview of the process:

Hardware:

- Acquire UWB RTLS devices: These devices consist of anchor nodes and tag nodes. Anchor nodes are stationary devices used for reference and positioning, while tag nodes are attached to objects or people whose location needs to be tracked.

- Install anchors: Mount the anchor nodes in strategic locations throughout the area where tracking will take place. The number of anchors required depends on the size of the area and desired accuracy. Typically, at least three anchors are needed, but more anchors can be used for improved precision.

- Connect anchors: Power up the anchor nodes using a suitable power source and establish a network connection between them. This allows them to communicate with each other and with the software application.

Software and Configuration:

- Install RTLS software: Obtain and install the appropriate RTLS software on a computer or server that will act as the central hub for the system. (Decawave DRTLS Manager)

- Configure the network: Set up the network parameters within the RTLS software, such as assigning unique IDs to each anchor and specifying their relative positions in the physical space. This information helps the system accurately calculate the position of the tag nodes.

Tag Node Deployment:

- Attach tag: Attach tag to the objects or individuals that need to be tracked. Ensure they are securely fastened and positioned for optimal signal reception.

- Activate tag nodes: Power on the tag nodes and configure them to communicate with the anchor nodes.

Data Collection and Analysis:

- Real-time tracking: Once the system is set up and the tag nodes are activated, the RTLS software will start receiving data from the tag nodes. The software will process the UWB signals received from the anchors and calculate the position of the tag nodes in real-time.
- Visualization and analysis: The RTLS software provides visualization tools to display the tracked locations on a map or floor plan. It may also offer additional features such as data logging, historical tracking, and integration with other systems.

By following these steps, you can implement an UWB RTLS and track the real-time location of objects or people within the designated area.

To set up the anchors for the Real-Time Location System (RTLS), follow these steps:

1. Start by selecting a few RTLS units to serve as anchors. While a minimum of three anchors is required for RTLS functionality, it is advisable to use at least four for improved accuracy.
2. Once you have identified the anchor units, proceed to mount them either on the wall or on tripods. Refer to the accompanying figure for visual guidance on the recommended placement.
3. It is recommended that set anchors at the same height.
4. Ensure the anchors are powered by connecting them to USB batteries or USB power supplies. This will provide the necessary electrical energy for their operation.

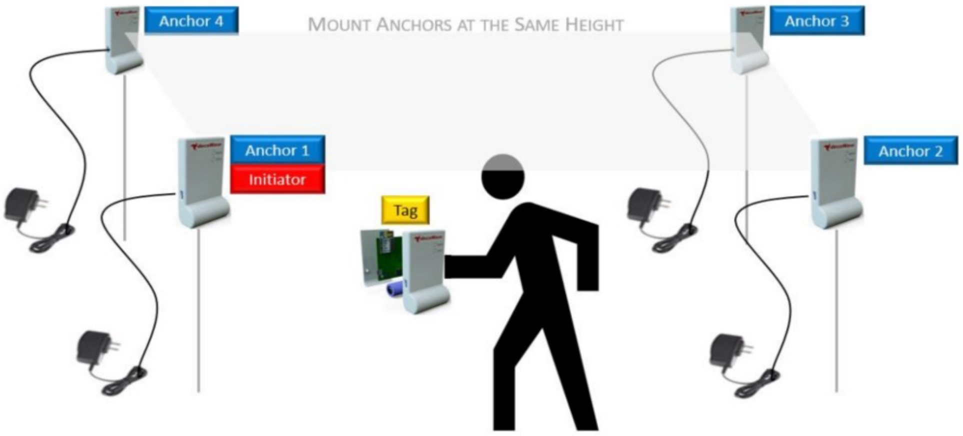

Figure 4: A schematic representing the measurement setup.

Prepare the Tags:

1. Select RTLS units to serve as tags. At least one tag is required for the system to function properly.
2. Battery Power:
    - Open the plastic enclosure of each tag unit.
    - Insert a rechargeable battery into the unit. The batteries are typically purchased separately.
    - Close the plastic enclosure to secure the battery in place.
3. USB Power Supply:
    - Alternatively, you can power the tags using a USB power supply or USB battery.
    - Connect the USB power supply or USB battery to the tags, providing them with the necessary power.

Prepare DRTLS manager software:

To download and install the "RTLS System Manager" application on your Android device, follow these steps:

1. Visit the Decawave website or the Google Play Store to obtain the latest Android .apk file for the "RTLS System Manager" application. You can access the Decawave website at https://www.qorvo.com/products/p/MDEK1001#documents.

2. Once you have downloaded the .apk file, locate it in the Downloads section of your Android device.
3. Tap on the downloaded .apk file to initiate the installation process. Your device may prompt you with a security warning about installing applications from unknown sources. If necessary, grant the required permission to proceed with the installation.
4. Follow the on-screen instructions to complete the installation of the "RTLS System Manager" application on your Android device. Once the installation is finished, you will find the application listed among your installed apps.

Computer system configuration:

To capture data directly to a PC, you can configure one of the devices as a listener. Here's a step-by-step guide on how to achieve this:

1. Set one of the RTLS units to PASSIVE mode. In this mode, the UWB functionality is enabled, but the RTLS unit does not actively participate in the network.
2. Connect a PC to the designated RTLS unit using a USB cable. Ensure the connection is properly established.
3. Open a shell terminal on the PC. This can be done through the command prompt or a terminal emulator, depending on the operating system.
4. In the terminal, type the command "les" (short for location-engine-show) to report the position of all the tags that the listener can hear. This command triggers the RTLS system to display the location information of the tags.
5. If you wish to save the data displayed in the terminal to a log file, you can redirect the output by appending the command with the appropriate parameters. For example, you can use the command "les > log.txt" to save the data to a file named "log.txt" in the current directory.
6. It's important to note that in this listener mode, only the position information of the tags is printed, and individual ranges are not included in the output.

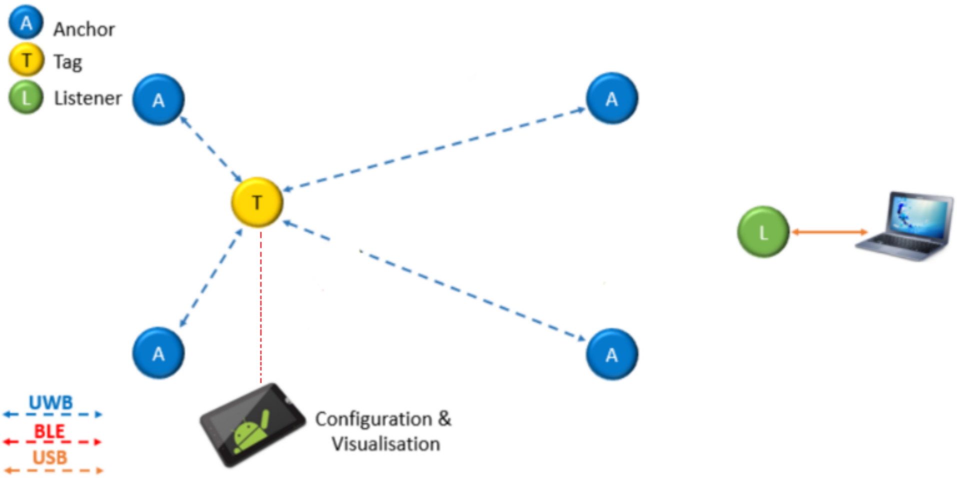

Figure 5: System Configuration Option: 4 Anchors, 1 Tag, 1 Listener

DRTLS Manager Usage Guide

Follow the steps below to get the DWM1001 Two-Way-Ranging Real Time Location System (DRTLS) up-and-running.

Android *Application:*

- Launch the Decawave DRTLS Manager application on your Android device.
- If no networks have been previously saved, the application will open on the home screen.
- If a network was previously saved, the application will open on the last viewed network screen.
- The home screen of the application will display the following information:
  - "Decawave DRTLS Manager" title.
  - Application version details.
  - A button labeled "Start Device Discovery" to initiate the device discovery process.
  - A button to navigate to the "Instructions" page, providing additional guidance.

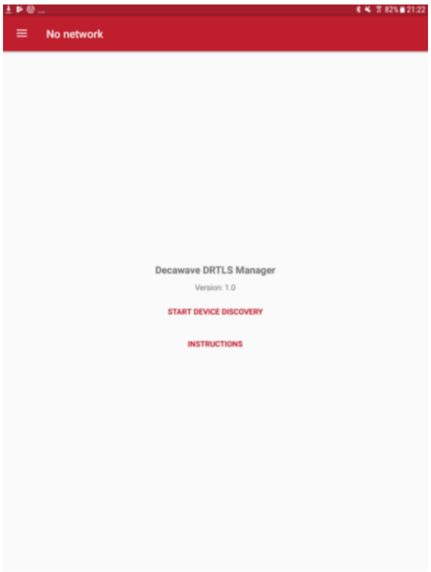

No network

Decawave DRTLS Manager

Version: 1.0

Figure 6: Decawave DRTLS Manager Home Screen

Start Device Discovery:

- Tap “Start Device Discovery”
- The application will automatically discover all devices that are in range and powered on
-

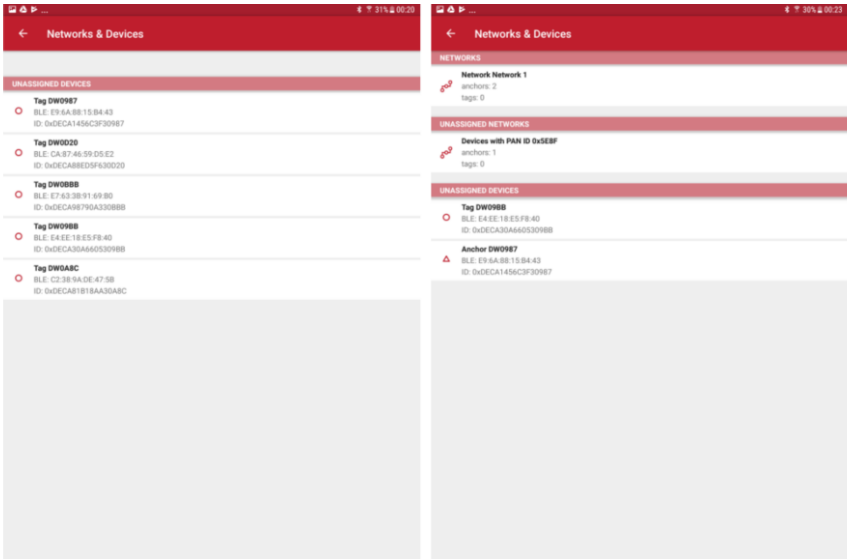

Networks & Devices

UNASSIGNED DEVICES

Tag DW0987
BLE: E9:6A:88:15:B4:43
ID: 0xDECA1456C3F30987

Tag DW0D20
BLE: CA:87:46:59:D5:E2
ID: 0xDECA88ED5F630D20

Tag DW0BBB
BLE: E7:63:3B:91:69:B0
ID: 0xDECA98790A330BBB

Tag DW09BB
BLE: E4:EE:18:E5:F8:40
ID: 0xDECA30A6605309BB

Tag DW0A8C
BLE: C2:38:9A:DE:47:5B
ID: 0xDECA81B18AA30A8C

Networks & Devices

NETWORKS

Network Network 1
anchors: 2
tags: 0

UNASSIGNED NETWORKS

Devices with PAN ID 0x5E8F
anchors: 1
tags: 0

UNASSIGNED DEVICES

Tag DW09BB
BLE: E4:EE:18:E5:F8:40
ID: 0xDECA30A6605309BB

Anchor DW0987
BLE: E9:6A:88:15:B4:43
ID: 0xDECA1456C3F30987

Figure 7: Device Discovery Screen

- Devices will be grouped into
  - ‘NETWORKS’
  - ‘UNASSIGNED DEVICES’

- ‘UNASSIGNED NETWORKS’

- The following information is shown under each device:

- Device Type (Anchor or Tag)
- Device Name in the form DW1234
- Network
- Bluetooth address
- Device ID

- The user can select a specific device by tapping an individual device

- The user will get the option to create a New Network name

- Alternatively, to select multiple devices:

- Tap-and-hold a single device
- The checkmark symbol (√) will be shown on the left of that device
- Other devices can be tapped and added to the selection
- Once selected, the button “ASSIGN” in the upper right-hand corner can be tapped to add these devices to a new (or existing) network

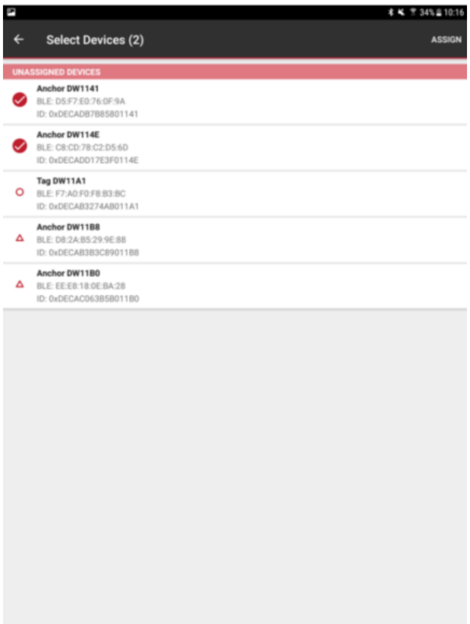

Anchor DW1141
BLE: D5:F7:E0:76:0F:9A
ID: 0xDECADB7B85801141

Anchor DW114E
BLE: C8:CD:78:C2:D5:6D
ID: 0xDECADD17E3F0114E

Tag DW11A1
BLE: F7:A0:F0:F8:B3:BC
ID: 0xDECAB3274AB011A1

Anchor DW11B8
BLE: D8:2A:B5:29:9E:88
ID: 0xDECAB3B3C89011B8

Anchor DW11B0
BLE: EE:E8:18:0E:BA:28
ID: 0xDECAC063B5B011B0

Figure 8: Device Discovery Screen – Select Multiple Device

Create a Network

- Name the Network e.g. “Waterpolo” and Tap ‘Save’
- Tap a network to see the list of devices in that network.

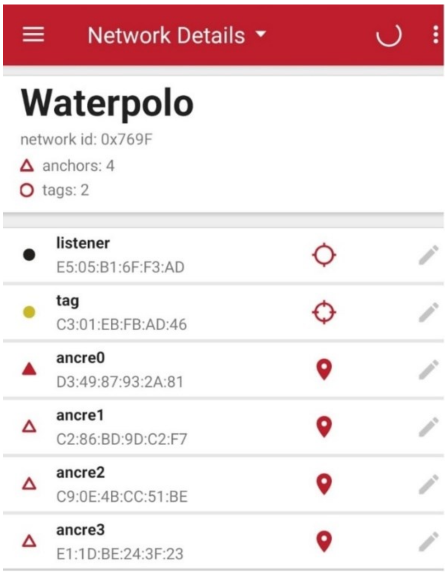

Waterpolo

network id: 0x769F
anchors: 4
tags: 2

●	**listener** E5:05:B1:6F:F3:AD
●	**tag** C3:01:EB:FB:AD:46
▲	**ancre0** D3:49:87:93:2A:81
△	**ancre1** C2:86:BD:9D:C2:F7
△	**ancre2** C9:0E:4B:CC:51:BE
△	**ancre3** E1:1D:BE:24:3F:23

Figure 9: Network Details Screen

Each device in the list shows information about that device

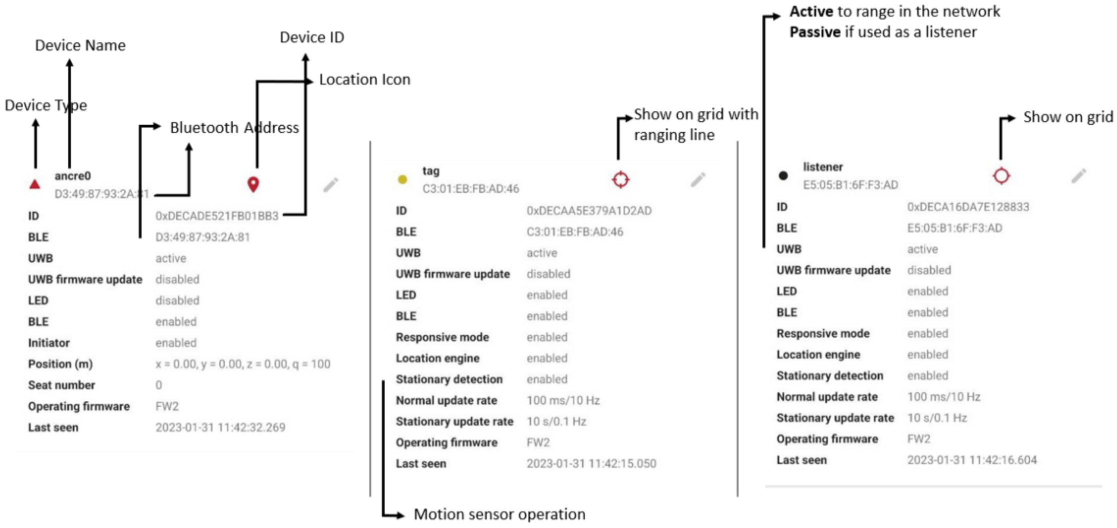

ancre0
D3:49:87:93:2A:81

ID	0xDECADE521FB01BB3
BLE	D3:49:87:93:2A:81
UWB	active
UWB firmware update	disabled
LED	disabled
BLE	enabled
Initiator	enabled
Position (m)	x = 0.00, y = 0.00, z = 0.00, q = 100
Seat number	0
Operating firmware	FW2
Last seen	2023-01-31 11:42:32.269

tag
C3:01:EB:FB:AD:46

ID	0xDECAA5E379A1D2AD
BLE	C3:01:EB:FB:AD:46
UWB	active
UWB firmware update	disabled
LED	enabled
BLE	enabled
Responsive mode	enabled
Location engine	enabled
Stationary detection	enabled
Normal update rate	100 ms/10 Hz
Stationary update rate	10 s/0.1 Hz
Operating firmware	FW2
Last seen	2023-01-31 11:42:15.050

listener
E5:05:B1:6F:F3:AD

ID	0xDECA16DA7E128833
BLE	E5:05:B1:6F:F3:AD
UWB	active
UWB firmware update	disabled
LED	enabled
BLE	enabled
Responsive mode	enabled
Location engine	enabled
Stationary detection	enabled
Normal update rate	100 ms/10 Hz
Stationary update rate	10 s/0.1 Hz
Operating firmware	FW2
Last seen	2023-01-31 11:42:16.604

Figure 10: Network Details Screen Device Information

- Device Type: A symbol to the left indicates the device type
  - Empty Triangle: Anchor
  - Filled Triangle: Initiator Anchor
  - Filled Circle: Tag. Each tag uses a different color
  - Black Circle: Listener
- Location icon: jumps to the grid screen and zooms to this anchor.
- The following parameters are displayed:
  - Device Name

- **ID:** Device ID
- **BLE:** Device Bluetooth address
- **NODE TYPE:** Set device to be either "Anchor" or "Tag". All devices will have a factory-default of 'tag' mode. Once the configuration is changed, and saved, the device will remember the new setting.
- **NETWORK:** Add the Node to a network (either a previously created network or, if none exists, the option to create a new network will appear)
- **UWB:** 'off', 'passive' or 'active'.
  - Set to 'active' to range in the network.
  - Set to 'passive' if used as a listener.

If in tag mode:

- **NORMAL UPDATE RATE:** Set the location update rate. The default is 10 Hz (calculates a location 10 times per second) but can be changed to other rates
- **STATIONARY UPDATE RATE:** Set the location update rate to be used when the device is stationary (detected by the motion sensor)
- **UWB FIRMWARE UPDATE:** Allows firmware update to propagate to this device
- **LED:** Disables/enables the LEDs on the board. May be used by a user to help identify which device is referenced.
- **STATIONARY DETECTION:** Enables/disables motion sensor operation. If disabled, then the stationary update rate will not be available.

If in anchor mode:

- **INITIATOR:** Configure this anchor as an initiator. At least one of the anchors must be an initiator in the network. The initiator will start and control the network.
- **POSITION**: The x, y, z co-ordinate of the anchor in the grid. Will be automatically populated if this device participated in auto positioning.
  - X position
  - Y position
  - Z position

Position the Anchors:

By using the Auto-Positioning Feature (for up to 4 anchors)

Note 1: The Auto-Positioning function is a quick setup feature to automatically determine the anchor locations. Note that this feature may result in a small error in anchor location, making reported tag locations less accurate. For best results it is recommended that anchor positions are measured to cm accuracy and manually entered. **Note 2:** Ensure Line-of-Sight between the anchors during these steps.

START: On the ‘Network Details’ screen Figure.6, tap the “Auto-Position” button in the upper right pull-down menu (anchors within Bluetooth range appear)

RE-ORDER: Re-order the anchors in the list to match their locations in the room:

- Order the anchors anti-clockwise in the room (as shown above)
- The 1st anchor in the list is the (0,0) coordinate

MEASURE: Tap “Measure” to start the auto-positioning

PREVIEW: Tap ‘PREVIEW’ to check locations before saving

SET HEIGHTS: Enter heights of the anchors by tapping ‘Z-AXIS’

SAVE: Save the anchors setup by tapping ‘SAVE’

- The location of the other anchors is calculated from the initial 3 anchor locations
- Errors will propagate through the anchors, so the usage is confined to small-scale systems e.g. up to 4 anchors
- Auto-positioning can only be used on the anchors that are within Bluetooth range of the android device.

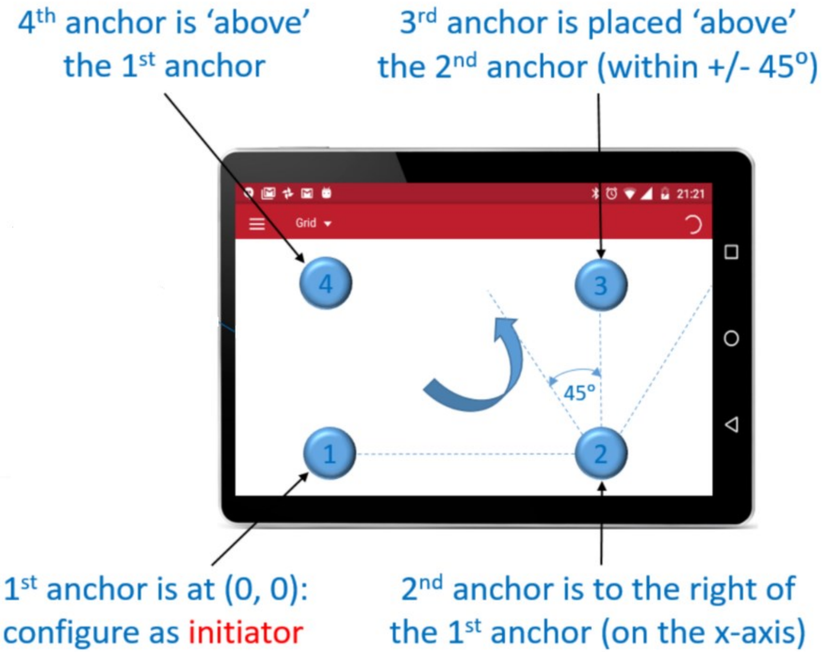

Figure 11: Auto-Positioning: Anchor Positioning Rules

- In turn, open each anchor’s device configuration screen.
- Enter the x, y, z co-ordinates of the anchors.

Logging Data via the USB Port

Tag location data can be logged using a USB connection instead of using the Android application. Note also that the PC terminal can be used to configure the anchors and tags – the Android application is not necessarily needed.

Instructions

- Setup the anchors and tags network via the Android application (see section 6)
- Download and install the J-Link software pack from Segger
- https://www.segger.com/downloads/jlink/#JLinkSoftwareAndDocumentationPack
- Download and install a common PC terminal program e.g. Tera Term http://download.cnet.com/Tera-Term/3000-2094_4-75766675.html
- Connect the tag to the PC via USB cable
- Open the device manager to identify what com port is assigned to the Tag, in this case COM20

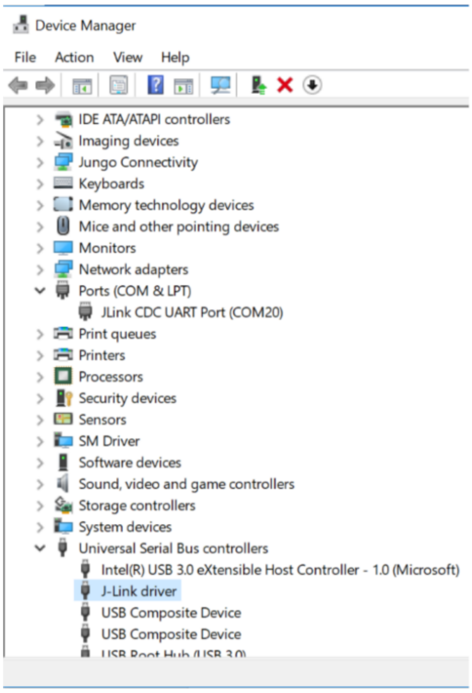

Figure 12: *J-Link driver on device manager*

- Once the com port has been identified open up Tera Term. Select the appropriate COM port as shown and set the terminal baud rate to 115200. The tag should now be connected.

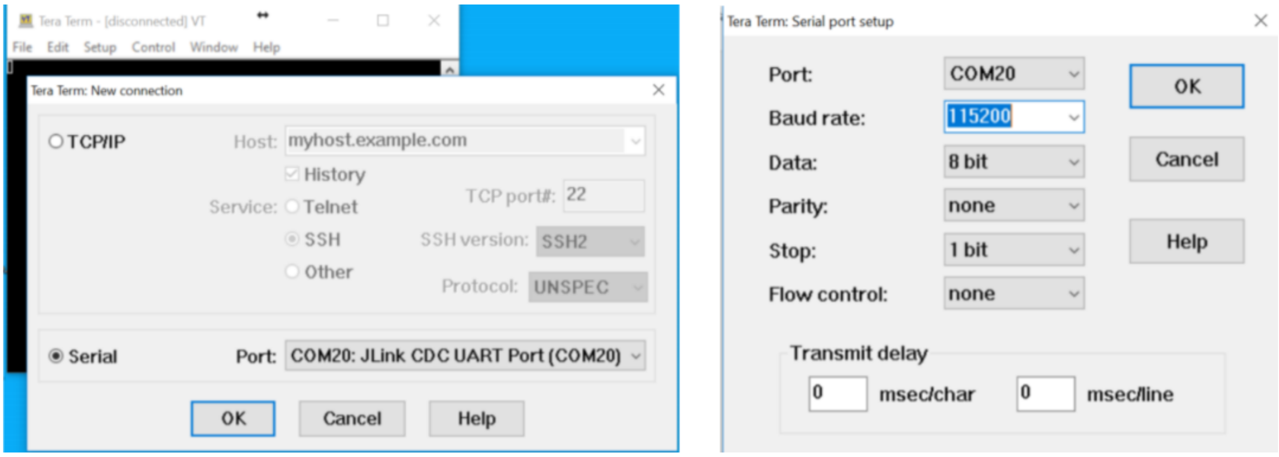

Tera Term: New connection

○ TCP/IP   Host: myhost.example.com
☑ History
Service: ○ Telnet   TCP port#: 22
● SSH   SSH version: SSH2
○ Other   Protocol: UNSPEC

● Serial   Port: COM20: JLink CDC UART Port (COM20)

Tera Term: Serial port setup

Port: COM20
Baud rate: 115200
Data: 8 bit
Parity: none
Stop: 1 bit
Flow control: none
Transmit delay
0 msec/char   0 msec/line

Figure 13: Tera Term Terminal setting

- Next press the PC Enter key two times and the prompt below appears:

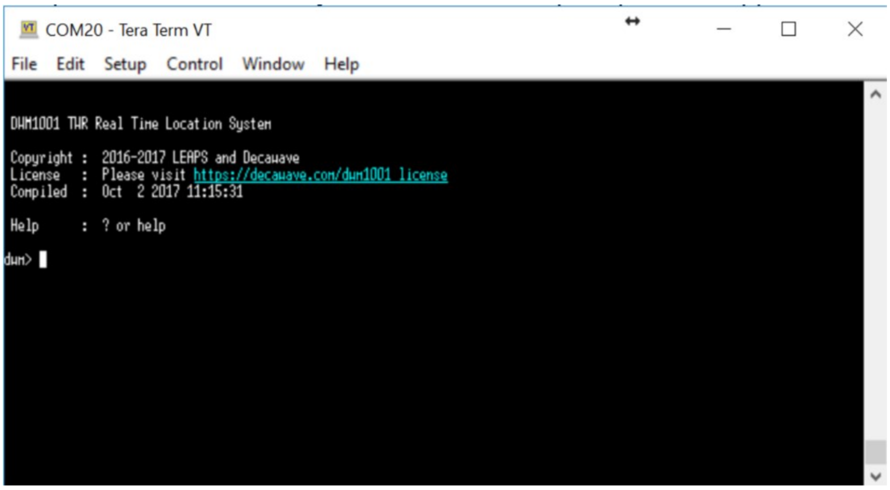

```
DWM1001 TWR Real Time Location System

Copyright :  2016-2017 LEAPS and Decawave
License   :  Please visit https://decawave.com/dwm1001_license
Compiled  :  Oct  2 2017 11:15:31

Help      :  ? or help

dwm> 
```

Figure 14: Tera Term Terminal

- Enter the command ‘nmt’ and press the return key **twice** which sets the tag into Active mode
- Enter ‘les’ to display the location estimates of the tag

CHAPTHER4: Experiments:

Experiment 1 (Innovation Lab):

The objective of the test is to evaluate several aspects related to the Real-Time Location System (RTLS) units and gather useful insights. The specific goals are as follows:

1. **Accuracy and Limitations of Auto-Positioning:** Assess the accuracy and limitations of the auto-positioning feature within the RTLS units. Determine how reliably the system can automatically determine the positions of anchors. Additionally, investigate any constraints or factors that may affect the performance of the auto-positioning functionality. This analysis helps in understanding the reliability and precision of the system's automated positioning capabilities.

2. **Manual Positioning:** Compare the results obtained from the auto-positioning mode with manually set positions. This involves manually configuring the positions of the anchors within the RTLS units. By comparing the accuracy and consistency of both approaches, it becomes possible to determine the most effective method for positioning the anchors. This analysis provides insights into whether manual positioning yields better results in terms of accuracy and reliability compared to auto-positioning.

3. **Mobile Application vs. Listener Results:** Compare and analyze the positioning results obtained from the mobile application with those obtained from the listener. This evaluation focuses on assessing the consistency and agreement between the two methods of capturing and reporting position data. By examining any discrepancies or similarities in the results, it becomes possible to identify potential variations or issues that may affect the accuracy and reliability of the results.

4. **Step Size Measurement**: Measure the time interval between data points to determine the step size within the RTLS units. This involves analyzing the frequency at which the system updates and provides new position data. By understanding the time intervals between data points, it becomes possible to assess the system's responsiveness and the rate at which it can track and report the movement of objects or individuals. This information is crucial for applications that require real-time tracking and monitoring.

The date and Duration of the Measurements:

On the specified date of 07/02/2023, the measurements for the test will be conducted from 9:00 until 18:00 at innovation lab in the Villejuif campus. The duration of the measurements varies depending on the number of points being tested and the time rates associated with each point. For each point, the test duration is approximately 2 minutes. This means that the total test time for all 11 points will be approximately 22 minutes. It is important to note that the number of measurements taken for each point may differ due to varying time rates associated with different points. The allocation of 2 minutes for each point allows for sufficient time to perform the necessary measurements and collect the required data.

Condition:

To illustrate the impact of the environment on UWB signals, Fig.15 shows the setup used for testing in the Innovation Lab. The environment includes various obstacles, such as walls and metallic elements, which can affect the propagation of UWB signals. Additionally, to minimize the effects of the floor on signal propagation, it is suggested to position the tags at a height of approximately one meter.

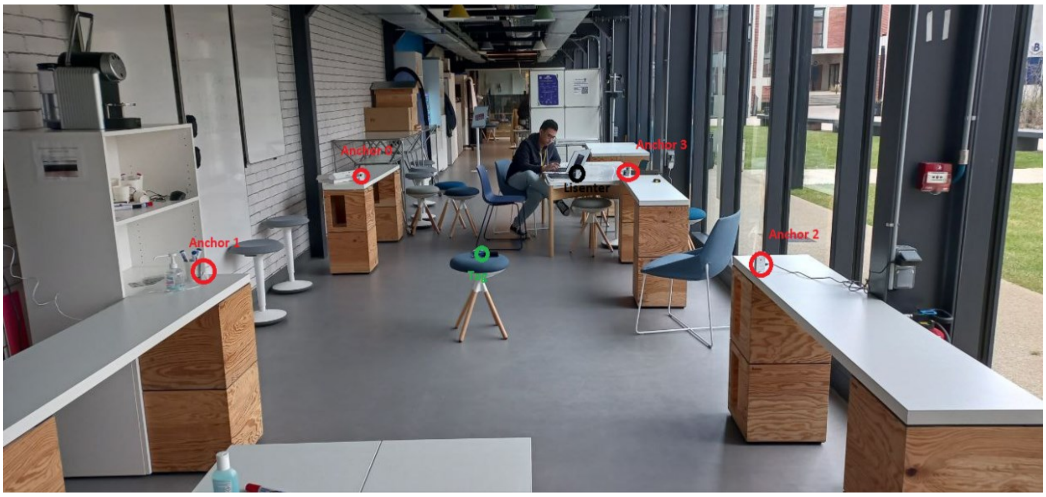

Figure 15: Photo of Innovation lab Environment

Fig.16 provides a visual representation of the experimental area used for the measurements. The dimensions of the area are 5.0 meters in length and 2.8 meters in width. The measurement points within this area are spaced at intervals of 0.5 meters, resulting in a total of 11 measurement points. In our experiment, we focus on measuring the middle line, which has a width of 1.4 meters. This line extends from the starting point at 0 meters and continues up to a length of 5 meters.

For this particular experiment, we employed a setup consisting of four units designated as anchors, one unit functioning as a tag, and an additional unit serving as a listener. The anchors play a crucial role in establishing the reference points within the real-time location system (RTLS), enabling accurate positioning and tracking of the tag unit. The tag unit, on the other hand, represents the object or individual being tracked throughout the experiment. Lastly, the listener unit is responsible for capturing and receiving the data transmitted by the anchors and tag unit, allowing for the analysis and evaluation of the system's performance. By utilizing this configuration, we were able to conduct comprehensive tests and gather data regarding the effectiveness and accuracy of the RTLS in tracking and positioning the tag unit in real-time.

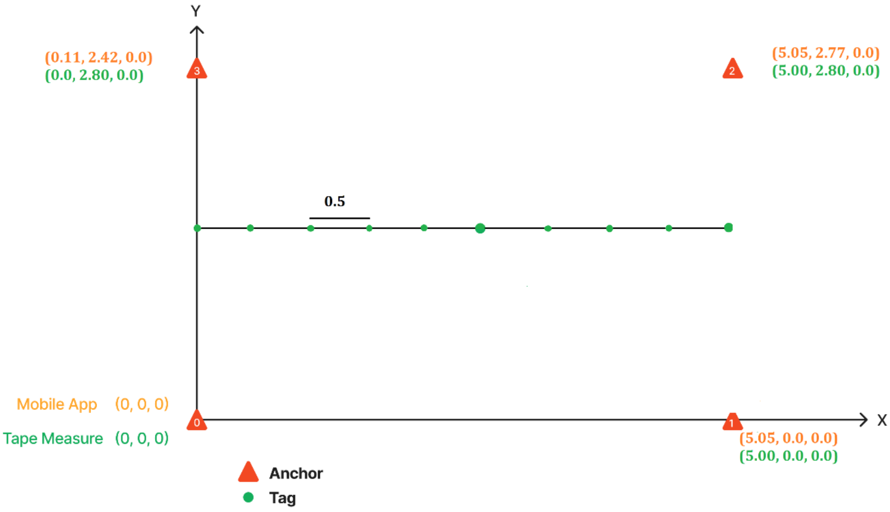

Figure 16: Schematic of Innovation lab experiment

In theory, manually setting the positions of anchors should yield more accurate results compared to automatic positioning. This is because when the application sets the positions of anchors automatically, there is a potential for error accumulation. The accumulated error can have a noticeable impact on the overall accuracy of the positioning system. To support this notion, Table.1 provides a clear demonstration of the error accumulation phenomenon. The table showcases the measured data, highlighting the differences between the auto positions and the actual positions. By comparing these values, the accumulated error becomes apparent, indicating a deviation from the desired accuracy. The manual positioning method, on the other hand, offers greater control and precision when setting the positions of anchors. By carefully determining the positions and minimizing the potential for error accumulation, the manual approach aims to achieve higher accuracy in the positioning system.

Table 1: Comparison of set anchors' position automatically and manually.

Anchor Number	True Position [m]	Auto-Positioning	Error [m]
0	[0.0, 0.0, 0.0]	[0.0, 0.0, 0.0]	00.0
1	[5.0, 0.0, 0.0]	[5.05, 0.0, 0.0]	0.05
2	[5.0, 2.8, 0.0]	[5.05, 2.77, 0.0]	0.0583
3	[0.0, 2.8, 0.0]	[0.11, 2.42, 0.0]	0.396

Data processing:

The data that is exported from listener consists of time, positions in three dimensions and tag quality. In this experiment we have 355 measurements for 11 points. Time intervals vary between 10 seconds and 0.1 seconds, which 0.1 seconds happened when the tag moves, and motion detector detects the movement. This allows for capturing more precise and frequent updates during periods of tag movement Fig.17.

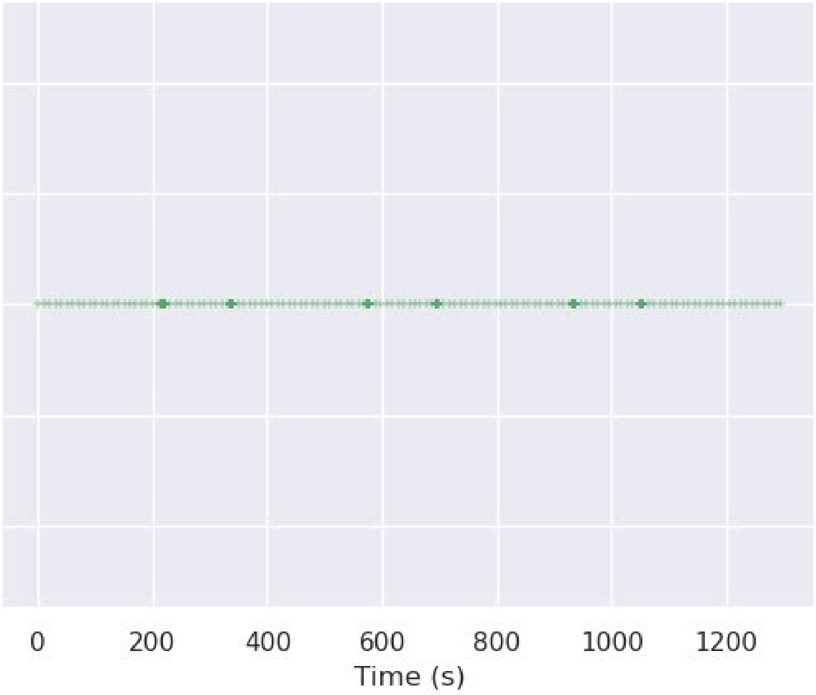

Figure 17: Time interval can be 10 or 0.1 seconds.

The scale of positions is millimeter, time is based on second, and tag quality is from 0 to 100. Tag quality is a measure of confidence of the accuracy of the location estimate based on the ranges received. Throughout the experiment, a total of 355 measurements were recorded, corresponding to 11 specific points. The time intervals between measurements vary depending on the circumstances Fig.18.

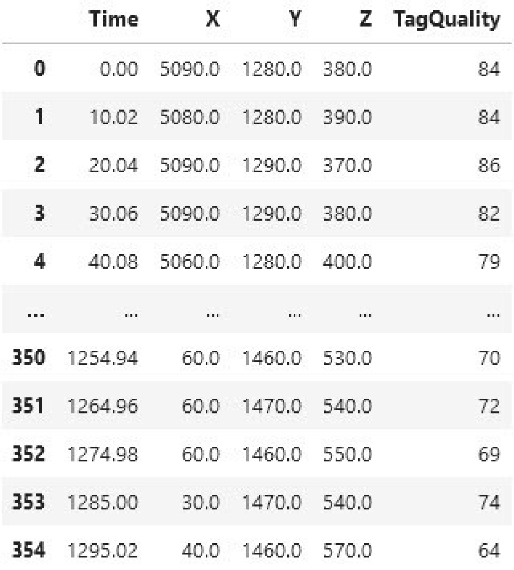

	Time	X	Y	Z	TagQuality
0	0.00	5090.0	1280.0	380.0	84
1	10.02	5080.0	1280.0	390.0	84
2	20.04	5090.0	1290.0	370.0	86
3	30.06	5090.0	1290.0	380.0	82
4	40.08	5060.0	1280.0	400.0	79
...	...	...	...	...	...
350	1254.94	60.0	1460.0	530.0	70
351	1264.96	60.0	1470.0	540.0	72
352	1274.98	60.0	1460.0	550.0	69
353	1285.00	30.0	1470.0	540.0	74
354	1295.02	40.0	1460.0	570.0	64

Figure 18: Data frame of measurements at innovation Lab

Fig.19 provides a visual comparison between two methods of setting anchor positions: automatic and manual in static mode. The purpose of this comparison is to assess the relative accuracy of the two approaches. By examining Fig.19, the differences in accuracy between the two methods become apparent. The data points or measurements depicted in the figure highlight the disparities between the desired or expected positions and the actual positions obtained using each method. It becomes evident that the manual positioning approach tends to exhibit greater proximity to the desired positions, indicating improved accuracy. The findings presented underscore the advantages associated with manual positioning. By carefully and precisely setting the anchor positions, we can minimize the likelihood of error accumulation and achieve a higher degree of accuracy in the positioning system.

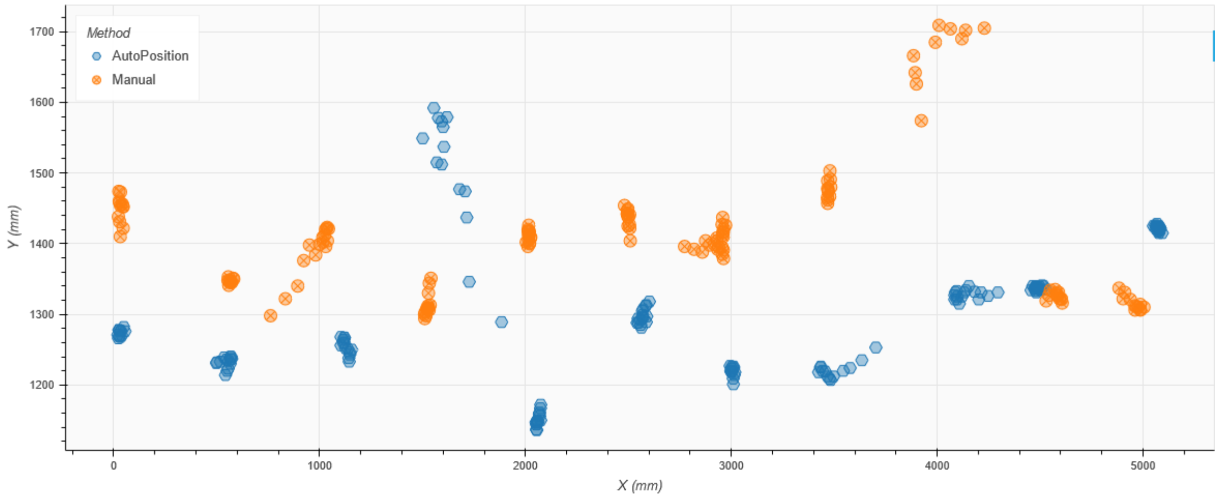

Figure 19: visual comparison between two methods of setting anchor positions: automatic and manual

These findings highlight the importance of considering the specific environmental factors and their potential impact on measurement accuracy. In this case, the floor's influence on the Z-axis measurements becomes a significant factor to be addressed in order to improve overall accuracy. Overall, the results indicate that measurements obtained through manual anchor positioning exhibit

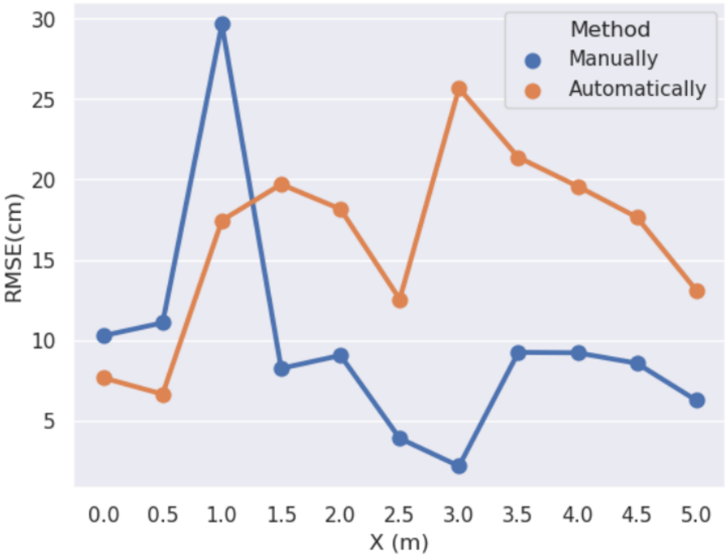

Figure 20: 2 Dimension RMSE for manual and Automatic methods

better accuracy compared to measurements obtained through automatic positioning, as depicted in Fig.20. The RMSE values serve as quantitative metrics for evaluating the level of accuracy achieved in each setting.

Fig.21 provides a visual representation of the cumulative distribution function (CDF) for both the manual and automatic methods. This CDF graph enables us to analyze the likelihood or probability of achieving certain levels of accuracy in the positioning system. As previously discussed, the manual method demonstrates superior performance in terms of accuracy. This is evident when examining the CDF curves for both methods. By examining the graph, we can observe that the manual method consistently outperforms the automatic method across various accuracy thresholds. Specifically, when considering a 90 percent likelihood or probability, the manual method achieves an accuracy of 11.08 centimeters. In contrast, the automatic method lags with an accuracy of 21.36 centimeters. On the other hand, the wider spread of the CDF curve for the automatic method indicates a greater degree of variability and potential inaccuracy in position estimation.

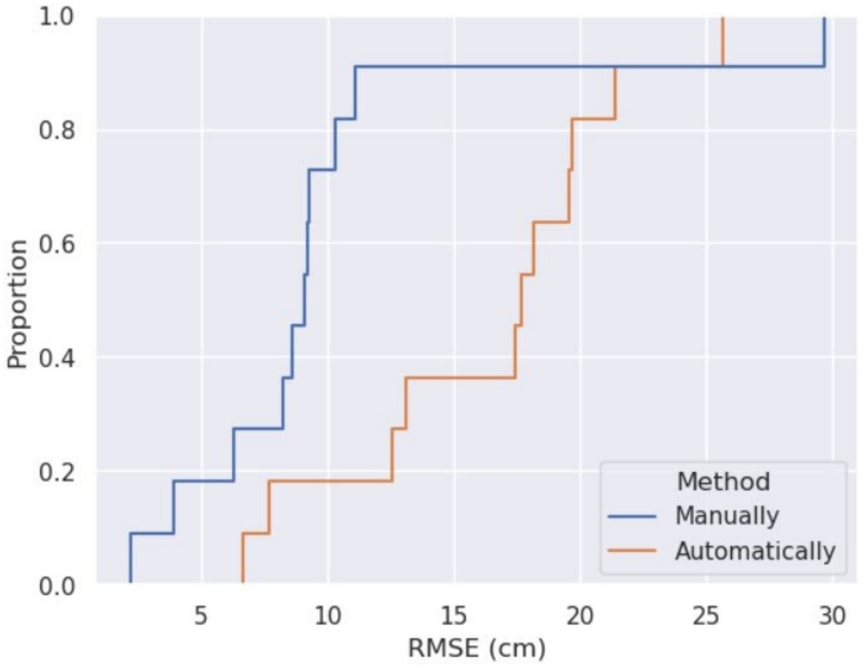

Figure 21: Cumulative distribution function for both the manual and automatic methods

Conclusion:

1. Manually setting anchor positions is more accurate than automatic positioning due to the potential for error accumulation.
2. The time intervals range from 100 milliseconds/10Hz to 10 seconds/0.1 Hz, offering two types of update rates: normal update rate and stationary update rate.
3. The results clearly demonstrate that manual positioning yields improved accuracy, as the manual approach consistently achieves greater proximity to the desired positions compared to the automatic method.

4. While the manual positioning method generally outperforms automatic positioning, it is important to acknowledge that there is a significant difference in accuracy for Z-axis measurements, with manual positioning exhibiting poorer performance due to signal reflections from the floor introducing complexities and inaccuracies in the measurement process.

5. The CDF analysis confirms that the manual method consistently outperforms the automatic method in terms of accuracy, with a significantly lower margin of error. The narrower spread of the CDF curve for the manual method demonstrates its higher reliability and precision in position estimation, highlighting its superiority over the automatic method.

6. Ultrawideband (UWB) signals are susceptible to various environmental factors that can impact their performance. These factors include physical obstacles like walls, floors, and other obstructions. When UWB signals encounter these obstacles, they undergo reflection, refraction, or diffraction, which can introduce distortions, signal attenuation, or multipath interference. For instance, in environments containing a high concentration of metal objects, such as industrial plants or buildings with steel frames, UWB signals may be reflected or absorbed by the metal surfaces. This can result in a weakening of the signal strength and degrade the overall performance of UWB technology.

Experiment 2 (Corridor floor 4 building A):

Objectives:

1. **Maximum Distance Between Anchors:** Determining the maximum distance between anchors is crucial for assessing the range and tracking capabilities of RTLS units. This measurement provides valuable insights into the system's ability to accurately monitor objects or individuals within a specific area. By establishing the maximum distance, it becomes possible to gain a comprehensive understanding of the system's coverage and limitations. This information is vital for making informed decisions regarding the design and deployment of the RTLS system, ensuring optimal performance and efficient utilization of resources.

2. **Conducting test in new environment:** Conducting test in new environment allows for an assessment of how obstacles impact the results of the RTLS system. By introducing various obstacles and studying their effects on signal propagation and accuracy, valuable insights can be gained. This information helps to identify potential challenges and limitations in different environments, enabling the development of strategies to overcome them. Understanding the impact of obstacles on the system's performance aids in fine-tuning the RTLS system, enhancing its reliability, and ensuring accurate tracking and positioning of objects or individuals in real-world scenarios.

3. **Performing test in the static mode:** Performing test in a static mode refers to conducting experiment where the objects or individuals being tracked remain stationary throughout the testing process. This type of testing allows for the assessment of the system's accuracy and precision in capturing and measuring static positions. By evaluating the system's performance under static conditions, valuable insights can be gained into its stability, consistency, and ability to provide reliable position data. This information aids in identifying any potential sources of error or deviation and helps in refining the system's algorithms or calibration processes to enhance its overall performance. Conducting tests in a static mode is an essential step in validating the reliability and accuracy of the tracking system before further evaluation in dynamic scenarios.

The date and Duration of the Measurements:

The scheduled test will take place on the specified date of 17/02/2023, between the hours of 8:00 and 13:00, specifically in the Forth floor’s corridor of building A located in the Villejuif campus. During the test, each point will be measured for approximately 100 seconds, with 10 acquisitions conducted per point at a time rate of 10 seconds. Both the anchor and tag units will be positioned at a consistent height of 80 centimeters, ensuring uniformity and consistency in the measurements taken throughout the experiment.

Condition:

In order to accurately measure the distance between two points, we designated one unit as an anchor and another unit as a tag. The anchor unit serves as a reference point while the tag unit is used to track and measure the distance from the anchor. However, it's important to consider the environmental factors that can impact the propagation of UWB signals. The test environment in this case includes various obstacles such as walls and metallic elements, which may affect the signal's path and accuracy. To mitigate the influence of the floor on signal propagation, it is recommended to position the tags at a height of approximately one meter.

It's worth noting that during the measurement, there was no interference from individuals or other objects as the test was conducted on a Saturday when the corridor was less likely to have regular foot traffic. Additionally, within the corridor, there are fire extinguishers positioned, one in the middle and another at the beginning. These objects can potentially affect signal propagation and should be taken into account when analyzing the measurement results. Moreover, the corridor is also equipped with several doors and large glass partitions, which could introduce additional reflections and signal distortions. These factors should be considered while interpreting the data and understanding any deviations or variations in the measurements. The designated area for our experiment spans 28.5 meters in length, 2 meters in width, and 2.4 meters in height. Within this area, we have established a grid-like structure of measurement points with a spacing of 0.5 meters between each point. This grid encompasses a total of 57 measurement points. Our primary focus lies on measuring the middle line, which runs along a width of 1 meter. Starting from the initial point at 0 meters, this line extends for a length of 28 meters, enabling us to analyze the data and draw insights specific to this central region Fig.22.

Figure 22: Photo of Forth floor's corridor of building A in the Villejuif campus

Data processing:

The dataset collected in this experiment comprises distance measurements and corresponding identifiers for each point. We have conducted a total of 570 measurements, covering 57 distinct points within the designated area. Each measurement point is sampled at a consistent time interval of 10 seconds, with 10 samples recorded for each point. Consequently, the total duration for capturing data at each point amounts to 100 seconds Fig.23. The output specifically focuses on the distance between the anchor and the tag, with distances being measured in meters. It is important to note that in this particular experiment, we did not include time or tag quality features as part of the data collection process. The resulting output file is formatted as a log file.

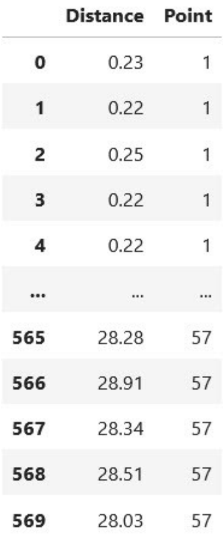

	Distance	Point
0	0.23	1
1	0.22	1
2	0.25	1
3	0.22	1
4	0.22	1
...	...	...
565	28.28	57
566	28.91	57
567	28.34	57
568	28.51	57
569	28.03	57

Figure 23: Data frame of measurements in the Corridor

To facilitate data processing, we selected a subset of the dataset consisting of intervals of 1 meter. Using only a portion of the data was sufficient for our analysis, and it allowed us to focus on specific segments of interest. In the next experiment, we will compare these results with the data obtained under interference conditions. Fig.24 provides a visual representation of the data frame, illustrating the measurements taken at each 1-meter interval with 10 samples per interval.

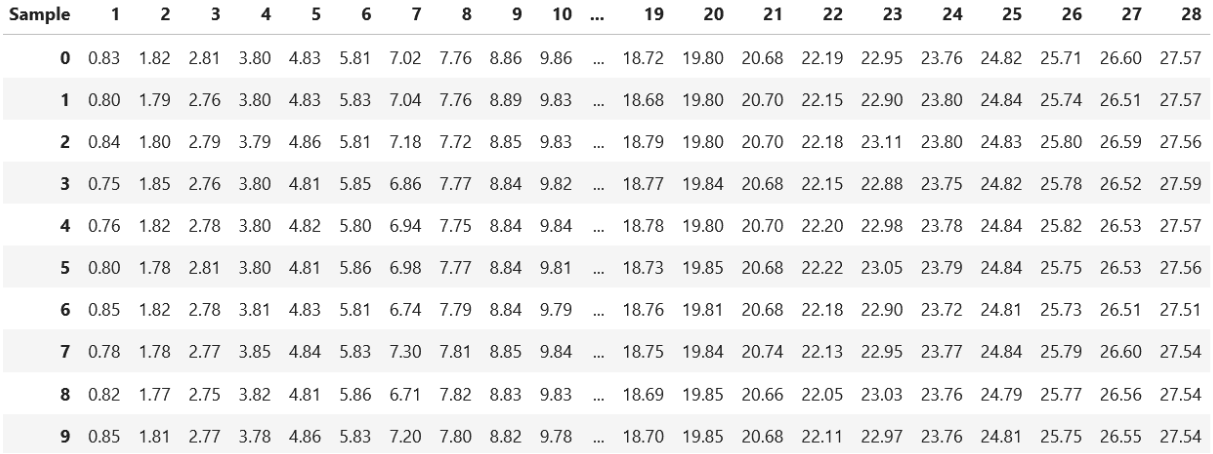

Sample	1	2	3	4	5	6	7	8	9	10	...	19	20	21	22	23	24	25	26	27	28
0	0.83	1.82	2.81	3.80	4.83	5.81	7.02	7.76	8.86	9.86	...	18.72	19.80	20.68	22.19	22.95	23.76	24.82	25.71	26.60	27.57
1	0.80	1.79	2.76	3.80	4.83	5.83	7.04	7.76	8.89	9.83	...	18.68	19.80	20.70	22.15	22.90	23.80	24.84	25.74	26.51	27.57
2	0.84	1.80	2.79	3.79	4.86	5.81	7.18	7.72	8.85	9.83	...	18.79	19.80	20.70	22.18	23.11	23.80	24.83	25.80	26.59	27.56
3	0.75	1.85	2.76	3.80	4.81	5.85	6.86	7.77	8.84	9.82	...	18.77	19.84	20.68	22.15	22.88	23.75	24.82	25.78	26.52	27.59
4	0.76	1.82	2.78	3.80	4.82	5.80	6.94	7.75	8.84	9.84	...	18.78	19.80	20.70	22.20	22.98	23.78	24.84	25.82	26.53	27.57
5	0.80	1.78	2.81	3.80	4.81	5.86	6.98	7.77	8.84	9.81	...	18.73	19.85	20.68	22.22	23.05	23.79	24.84	25.75	26.53	27.56
6	0.85	1.82	2.78	3.81	4.83	5.81	6.74	7.79	8.84	9.79	...	18.76	19.81	20.68	22.18	22.90	23.72	24.81	25.73	26.51	27.51
7	0.78	1.78	2.77	3.85	4.84	5.83	7.30	7.81	8.85	9.84	...	18.75	19.84	20.74	22.13	22.95	23.77	24.84	25.79	26.60	27.54
8	0.82	1.77	2.75	3.82	4.81	5.86	6.71	7.82	8.83	9.83	...	18.69	19.85	20.66	22.05	23.03	23.76	24.79	25.77	26.56	27.54
9	0.85	1.81	2.77	3.78	4.86	5.83	7.20	7.80	8.82	9.78	...	18.70	19.85	20.68	22.11	22.97	23.76	24.81	25.75	26.55	27.54

Figure 24: a subset of the dataset consisting of intervals of 1 meter

In order to further analyze and assess the accuracy of the measurements, we computed the absolute error for each sample and data point. This metric allows us to quantify the disparity between the obtained measurements and the expected values. Fig.25 provides a comprehensive depiction of the absolute error associated with each measurement. The figure presents key statistical metrics such as the number of samples, the mean, standard deviation, minimum, and maximum values for each measurement point. By examining these metrics, we gain a deeper understanding of the variability and spread of the absolute error across different points.

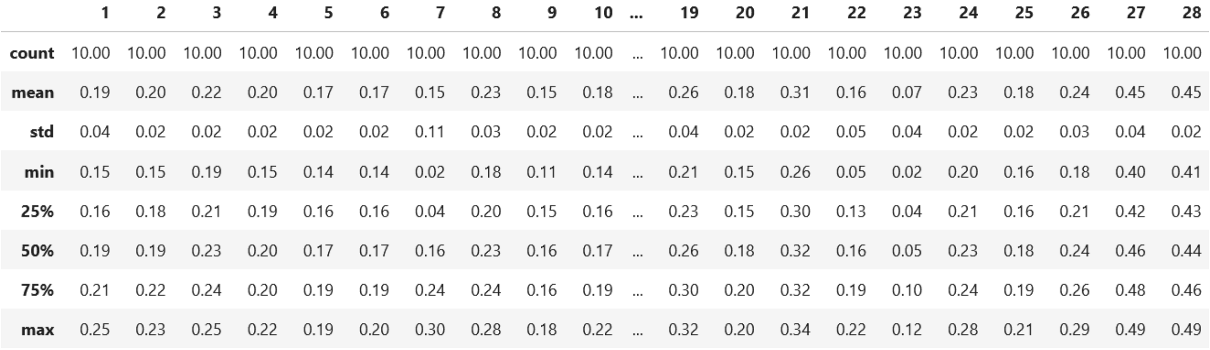

	1	2	3	4	5	6	7	8	9	10	...	19	20	21	22	23	24	25	26	27	28
count	10.00	10.00	10.00	10.00	10.00	10.00	10.00	10.00	10.00	10.00	...	10.00	10.00	10.00	10.00	10.00	10.00	10.00	10.00	10.00	10.00
mean	0.19	0.20	0.22	0.20	0.17	0.17	0.15	0.23	0.15	0.18	...	0.26	0.18	0.31	0.16	0.07	0.23	0.18	0.24	0.45	0.45
std	0.04	0.02	0.02	0.02	0.02	0.02	0.11	0.03	0.02	0.02	...	0.04	0.02	0.02	0.05	0.04	0.02	0.02	0.03	0.04	0.02
min	0.15	0.15	0.19	0.15	0.14	0.14	0.02	0.18	0.11	0.14	...	0.21	0.15	0.26	0.05	0.02	0.20	0.16	0.18	0.40	0.41
25%	0.16	0.18	0.21	0.19	0.16	0.16	0.04	0.20	0.15	0.16	...	0.23	0.15	0.30	0.13	0.04	0.21	0.16	0.21	0.42	0.43
50%	0.19	0.19	0.23	0.20	0.17	0.17	0.16	0.23	0.16	0.17	...	0.26	0.18	0.32	0.16	0.05	0.23	0.18	0.24	0.46	0.44
75%	0.21	0.22	0.24	0.20	0.19	0.19	0.24	0.24	0.16	0.19	...	0.30	0.20	0.32	0.19	0.10	0.24	0.19	0.26	0.48	0.46
max	0.25	0.23	0.25	0.22	0.19	0.20	0.30	0.28	0.18	0.22	...	0.32	0.20	0.34	0.22	0.12	0.28	0.21	0.29	0.49	0.49

Figure 25: description of absolute error of measurements

The root mean square error (RMSE) diagram provides valuable insights into the overall accuracy of the measurements. Upon analysis, it is observed that the majority of errors are around 20 cm, indicating a relatively consistent level of accuracy across most positions. However, there is a significant increase in error at position x = 14 m, where the RMSE reaches 45 cm. This notable deviation from the average error suggests the presence of a metal obstacle in the environment, which could be causing signal reflections or interference, leading to a higher level of error in that specific location. On the other hand, the minimum RMSE is observed at position x = 23 m, with an error of only 7 cm. This indicates a high level of accuracy and precision in estimating the position at that particular point. The discrepancy between the minimum and maximum RMSE values

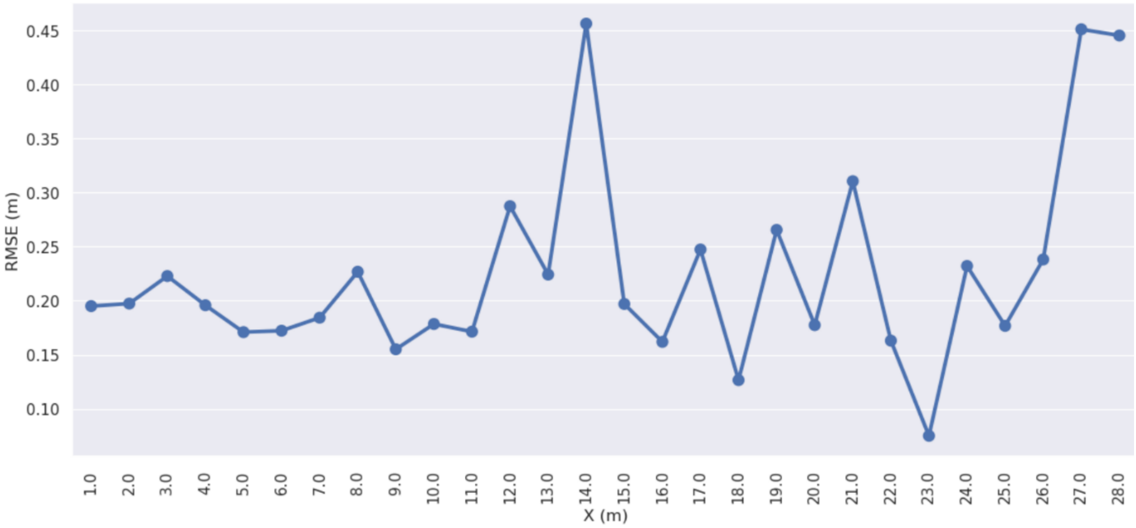

Figure 26: root mean square error (RMSE) diagram of distance measurement.

highlights the impact of environmental factors, such as obstacles, on the overall performance and accuracy of the measurement system Fig.26.

In Fig.27, we observe the root mean square error (RMSE) as well as the minimum and maximum error for each point in one figure. The figure reveals that the majority of results exhibit a similar level of variance, with a standard deviation of approximately 2.5 cm. This indicates a consistent and reliable estimation of the distances in those areas. However, there are two points that deviate from this pattern. Position x=7 demonstrates the highest variance with a standard deviation of 11 cm, suggesting a greater level of uncertainty and variability in the measurements taken at that specific location. On the other hand, position x=14 exhibits the lowest variance with a standard deviation of 2 cm.

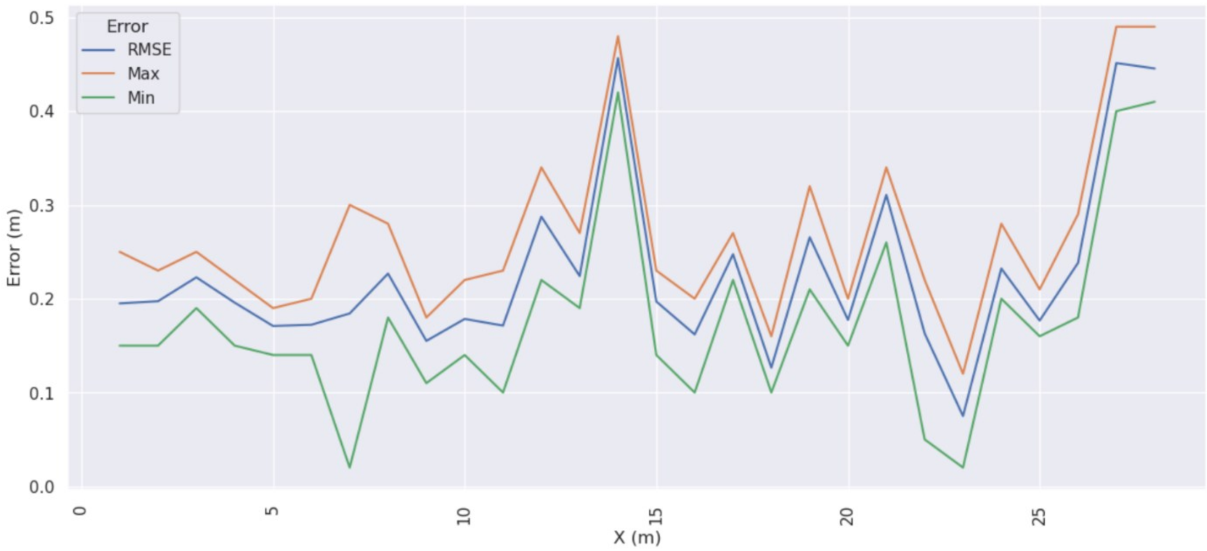

Figure 27: RMSE, minimum, and maximum error for each point in distance measurement

The cumulative distribution function (CDF) plot of the test results provides valuable insights into the distribution and accuracy of the measurements. From the CDF, we can determine the percentage of measurements that fall within certain RMSE thresholds. In this case, the CDF reveals that 50% of the measurements have an RMSE less than 20 cm. Furthermore, the CDF demonstrates that 90% of the measurements have an RMSE less than 30 cm, indicating that the majority of the measurements exhibit a reasonable level of accuracy within this threshold Fig.28.

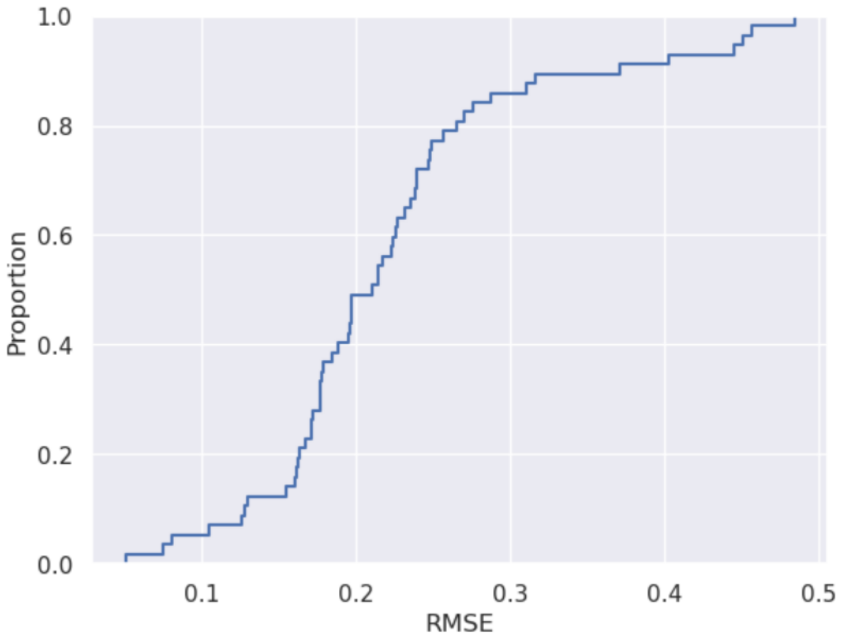

Figure 28: cumulative distribution function (CDF) plot of the test

Experiment 3 (Corridor floor 4 building A):

Objectives:

In this experiment, we aim to replicate the same scenario as the previous experiment while introducing an additional factor: the simultaneous use of Bluetooth technology. By conducting measurements in the presence of both Ultra-Wideband (UWB) and Bluetooth signals, we seek to investigate and analyze any potential interferences or impacts on the performance of the positioning system. This will provide valuable insights into the compatibility and coexistence of UWB and Bluetooth technologies in real-world scenarios, helping us understand the extent of any signal interferences and their effects on the accuracy and reliability of the system. By comparing the results from this experiment with those obtained from the previous one, we can gain a better understanding of the influence of Bluetooth technology on the UWB-based positioning system.

While it is theoretically expected that the DWM1001-DEV board, utilizing the Ultra-Wideband (UWB) transceiver development kit, operates at a frequency of 6.5 GHz, and Bluetooth operates at 2.4 GHz, indicating minimal or no interference between the two technologies, it is essential to validate this assumption Fig.29. In this test, our objective is to ensure and confirm the absence of interference between Bluetooth and UWB, while also exploring the feasibility of simultaneous usage of both

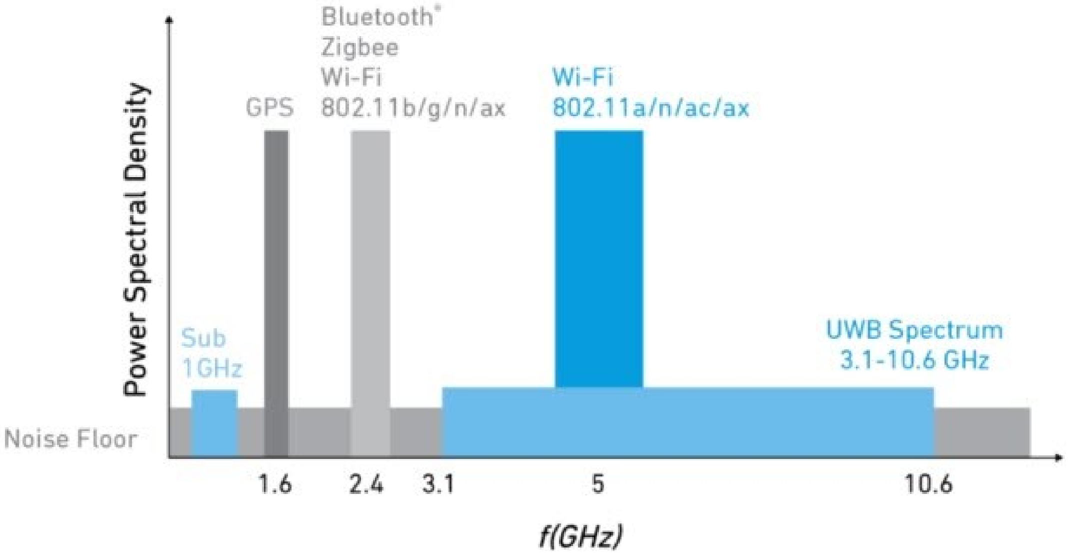

Figure 29: UWB Frequency coexists with other wireless technologies.

technologies. By conducting this experiment, we can assess the coexistence and compatibility of Bluetooth and UWB, providing valuable insights for potential applications requiring the concurrent utilization of these technologies.

The date and Duration of the Measurements:

The designated test is scheduled to be conducted on the assigned date of 19/04/2023, encompassing a time frame from 18:00 to 20:00. The chosen location for the test is the corridor on the Forth floor of building A within the Villejuif campus. Throughout the duration of the test, each measurement point will undergo observation for approximately 100 seconds, with a total of 10 acquisitions made per point at a time interval of 10 seconds.

Conditions:

To ensure consistency and accurate comparison of results, the test will be conducted in a single environment using the same measurement configuration. The chosen location is the corridor on the fourth floor of building A at Villejuif campus, which offers a maximum length of 28 meters. The measurements will be taken at regular intervals of 1 meter, capturing data points along the corridor. For the Ultra-Wideband (UWB) measurements, 10 samples will be taken at each point, reflecting a time rate specific to UWB technology. On the other hand, for the Bluetooth measurements, 30 samples will be collected at each point, accounting for the different time rates associated with Bluetooth technology Fig.24.

Figure 30: Forth floor's corridor of building A in the Villejuif campus will be obtained to conduct the interference test.

The test will be conducted in three distinct scenarios. Firstly, measurements will be taken solely using the UWB technology. Secondly, the test will focus solely on Bluetooth technology. Lastly, both UWB and Bluetooth devices will be employed simultaneously to examine their performance in a shared environment. This comprehensive approach allows for a thorough evaluation of each technology's individual performance as well as their potential interference when used concurrently. Throughout the experiment, all anchor and tag positions will remain constant, maintaining the same coordinates (x, y, z) for accurate comparison and analysis.

Data processing:

As depicted in Figure 31, our hypothesis that there would be no interference between Ultra-Wideband (UWB) and Bluetooth signals has been confirmed. However, slight differences or shifts observed in the results can be attributed to environmental factors. It is important to note that during the UWB and Bluetooth test, the presence of individuals crossing the signal path may have influenced the outcomes. Therefore, while the interference between UWB and Bluetooth signals was minimal, the impact of environmental variables and human presence should be considered when interpreting the observed differences in the results.

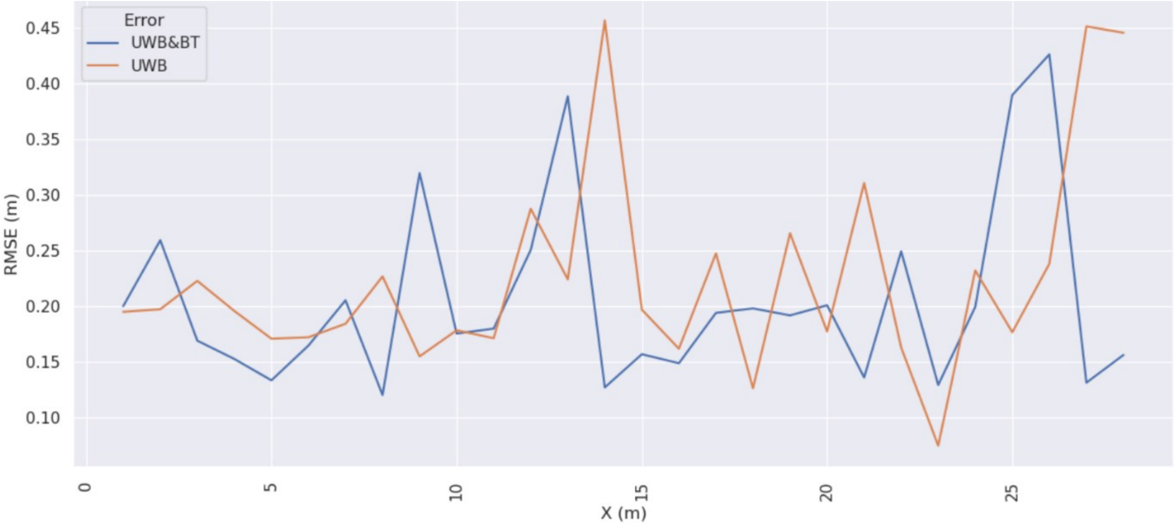

Figure 31: Comparing RMSE for both tests (UWB and UWB&BT)

Figure 32, which presents the cumulative distribution functions of both scenarios, provides further confirmation that there is no interference between UWB and Bluetooth technologies. The fact that the two graphs exhibit considerable overlap indicates that the performance of UWB and Bluetooth signals remains unaffected by each other. This overlap in the cumulative distribution functions suggests that the two technologies can coexist without significantly impacting each other's functionality or performance.

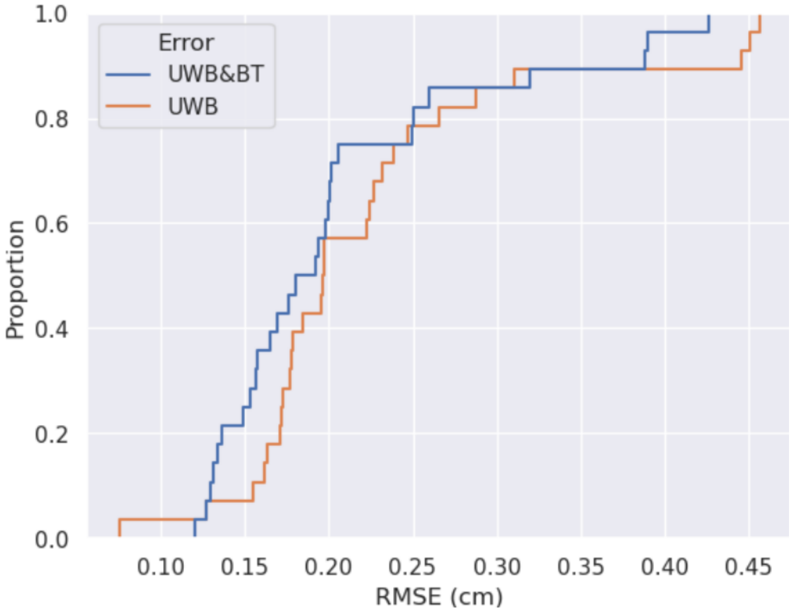

Figure 32: Comparing CDF for both tests (UWB and UWB&BT)

Upon conducting a thorough comparison of the results obtained from UWB measurements in both scenarios, with and without Bluetooth, it is evident that no interference exists between the two technologies. To further evaluate their performance, we compared the measurements of UWB and Bluetooth in a static mode within identical environments. Figure 33 illustrates that UWB exhibits greater reliability and precision compared to Bluetooth in our specific case study. The UWB measurements demonstrate an average error of approximately 20 centimeters with low variance, highlighting its consistent accuracy. Conversely, Bluetooth exhibits higher variance and error rates. It is worth noting that two different algorithms were employed: Bluetooth High precision and IFFT (Inverse Fast Fourier Transform). These findings emphasize the superior performance and precision of UWB over Bluetooth in the context of our study.

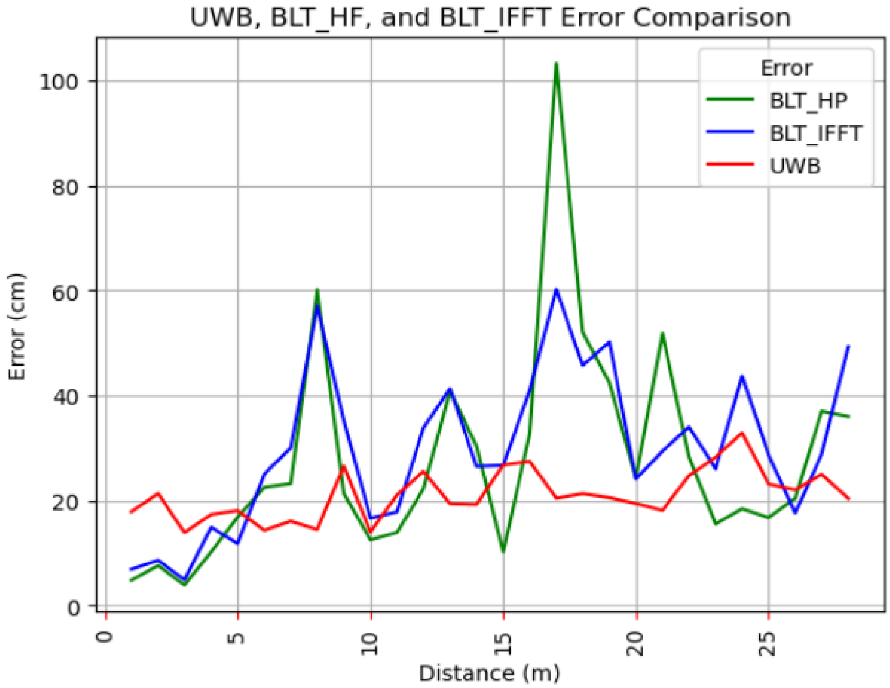

Figure 33: Error comparison between two technologies UWB and Bluetooth

Conclusions:

- There is no interference between UWB and Bluetooth technologies: The study confirms that there is no mutual interference observed between UWB and Bluetooth technologies. This implies that these two technologies can coexist without impacting each other's functionality.

- UWB outperforms Bluetooth in this case study: The results indicate that UWB technology exhibits superior performance compared to Bluetooth in the specific case study. UWB demonstrates better accuracy, precision, and reliability in the measurements conducted.

- Distinctions between UWB results with and without Bluetooth interference are attributed to external factors: Any observed distinctions between the UWB results with and without Bluetooth interference can be attributed to external factors. These factors may include situations such as walking, where movement or the presence of individuals may introduce interference. Additionally, human error in the placement of tags or devices can also contribute to variations in the results.

Experiment 4 (Gymnasium):

Objectives:

- **Test different scenarios to observe changes in results**: The study aims to examine various scenarios, including walking, running, running at an increased speed compared to the previous scenarios, and a combination of sprinting, walking, and running. By testing these different scenarios, the goal is to assess any potential variations or effects on the results. This analysis provides insights into how different activities impact the performance of the system being studied, and its ability to accurately estimate positions throughout the diverse locomotion scenarios.

- **Test a new environment and configuration setup**: The study intends to evaluate the performance of the system in a new environment, which may differ in terms of physical characteristics, infrastructure, or interference sources compared to previous settings. Additionally, a new configuration setup is tested, which may involve adjustments in hardware, placement, or parameters. By conducting these tests, the study aims to assess the system's adaptability and performance in different environments and configurations.

- **Experiment with both static and dynamic methods**: The objective is to explore and compare the results obtained from both static and dynamic methods. Static methods involve measurements or observations in stationary or controlled conditions, while dynamic methods capture data during motion or changing conditions. By conducting experiments using both approaches, the study seeks to understand the impact of motion and dynamics on the system's performance and compare it with the results obtained under static conditions.

- **Compare scenarios to investigate changes**: The objective is to compare the outcomes of the different scenarios and investigate any observable changes. By conducting a comparative analysis, the study aims to identify patterns or differences in the results. This comparison provides valuable information on how variations in scenarios affect the measured parameters and helps understand the system's behavior under different conditions.

- **Exploring the System's Capabilities and Limitations Across Diverse Locomotion Scenarios:** These four scenarios provide a comprehensive range of movements and speeds, allowing researchers to assess the system's performance and accuracy in capturing and estimating the trajectory under different conditions. By incorporating variations in speed and movement patterns, the experiment aims to provide valuable insights into the system's capabilities and limitations across different locomotion scenarios.

The date and Duration of the Measurements:

The scheduled test is planned to be conducted on the specified date of 22/05/2023, within a time frame from 13:00 to 18:00. The test location is set to be the Gymnasium in Villejuif. This designated venue provides a suitable environment for carrying out the test, ensuring the availability of the necessary facilities and space required for the planned activities.

Condition:

The experiment conducted in this study covered an area measuring 20 meters by 28 meters. The positions of the anchors were determined as follows: [9.0, 0.0, 1.5], [18.0, 0.0, 1.5], [18.0, 20.0, 1.5], and [9.0, 20.0, 1.5]. The path chosen for testing was along the line Y = 8 meters, which spanned a length of 28 meters. All four scenarios were performed within this configuration Fig.34.

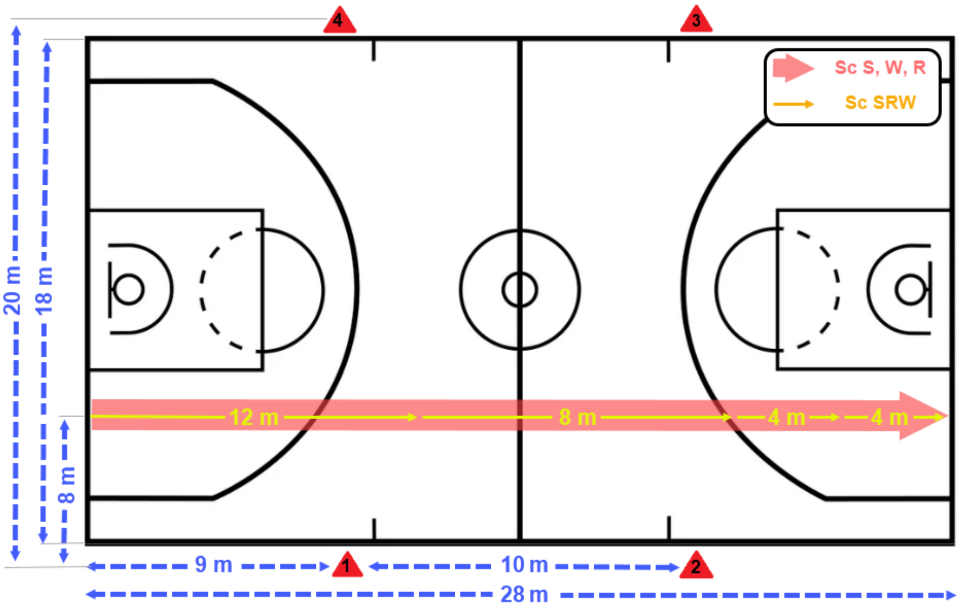

Figure 34: Schematic of setup configuration with movement scenarios

The experiment consists of four distinct scenarios. The first scenario involves walking at a constant speed along the designated line. In this scenario, participants maintain a consistent walking pace throughout the 28-meter path. The second scenario focuses on running along the 28-meter line. Participants are instructed to run at a steady pace throughout the entire distance, covering the designated path with continuous running movements. The third scenario replicates the previous running scenario but with a higher speed. Participants are required to run at an increased pace along the same 28-meter line. The fourth and final scenario is a combination of different movements. Participants begin by accelerating for the first 12 meters of the path, gradually gaining speed. Following this acceleration phase, participants decelerate for the next 8 meters, gradually reducing their speed. Then, participants transition into walking for the subsequent 4 meters, maintaining a steady walking pace. Finally, for the last 4 meters of the path, participants are instructed to run, completing the scenario.

These four scenarios provide a comprehensive range of movements and speeds, allowing researchers to assess the system's performance and accuracy in capturing and estimating the trajectory under different conditions. By incorporating variations in speed and movement patterns, the experiment aims to provide valuable insights into the system's capabilities and limitations across different locomotion scenarios.

Figure 35: Gymnasium environment in Villejuif to implement the dynamic experiment

It is important to note that this test was conducted in a dynamic scenario, meaning there was no specific benchmark point available to calculate position error. However, since the tests were conducted along the Y = 8 meters line, the trajectory error could be computed based on this line as a reference. The time rate of measurement during the experiment was set at 10 Hz, meaning there were 10 samples taken per second. This sampling frequency provided a sufficient rate of data acquisition to capture the necessary information for analysis and evaluation.

Data processing:

First scenario walking:

The first scenario involved walking along the designated line. A total of 102 samples were collected during the test, with a testing duration of 13.52 seconds to cover the entire 28-

meter path. Figure 36 provides a graphical representation of the data collected in this scenario, along with descriptive statistics including the minimum, maximum, mean, and standard deviation. The collected data and associated statistics offer valuable insights into the performance and variability of the measurements obtained during the walking scenario.

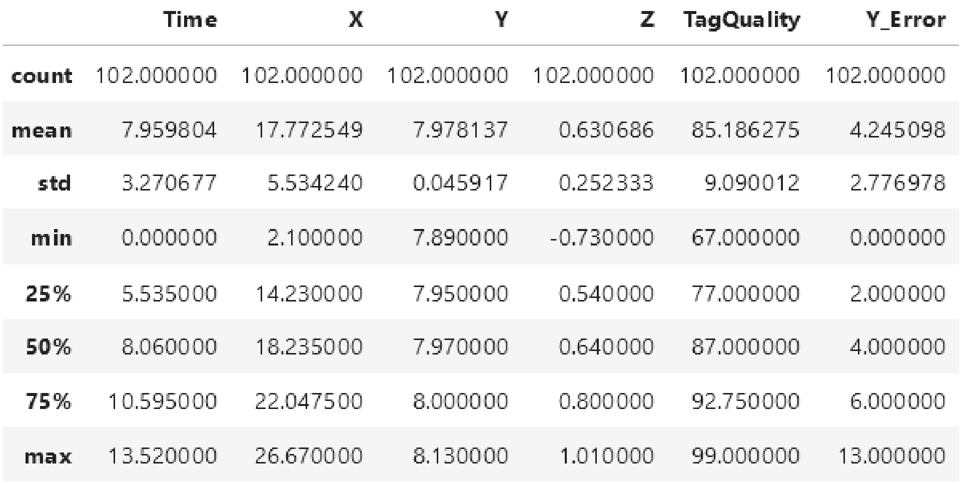

	Time	X	Y	Z	TagQuality	Y_Error
count	102.000000	102.000000	102.000000	102.000000	102.000000	102.000000
mean	7.959804	17.772549	7.978137	0.630686	85.186275	4.245098
std	3.270677	5.534240	0.045917	0.252333	9.090012	2.776978
min	0.000000	2.100000	7.890000	-0.730000	67.000000	0.000000
25%	5.535000	14.230000	7.950000	0.540000	77.000000	2.000000
50%	8.060000	18.235000	7.970000	0.640000	87.000000	4.000000
75%	10.595000	22.047500	8.000000	0.800000	92.750000	6.000000
max	13.520000	26.670000	8.130000	1.010000	99.000000	13.000000

Figure 36: Description of the data collection during walking scenario

Figure.37 provides a visual representation of the collected data, offering a comprehensive perspective on the dataset. The visualization includes the data samples, anchors, and the line path, providing a clear depiction of their spatial arrangement. By examining the figure, we can observe variations in the density of data samples along the line path. Certain areas exhibit a higher concentration of data samples, while other areas appear sparser. This variation in sample density may be attributed to various factors, such as the presence of metal objects in the environment or the specific experimental setup employed during the data collection process.

The presence of metal objects in the environment can affect the propagation of signals and impact the accuracy and reliability of the measurements. Objects with high conductivity, such as metal, can cause signal reflections, multipath interference, or signal attenuation, leading to variations in the observed sample density along the line. Additionally, the experimental setup itself can contribute to variations in sample density. Factors such as the placement and configuration of the anchors, the positioning of the data sampling devices, or the selection of measurement techniques can influence the spatial distribution of the collected data.

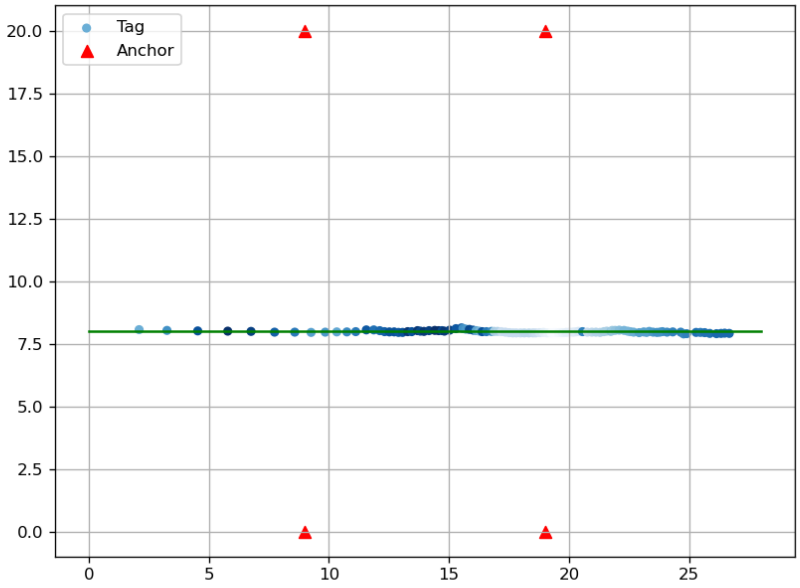

Figure 37: Visualization of first scenario walking

The trajectory error is a metric used to evaluate the accuracy of a predicted or estimated trajectory compared to a ground truth or reference trajectory. It quantifies the deviation or difference between the actual path taken by an object or entity and the expected or desired path. The trajectory error in this study was found to be less than 13 centimeters, with the majority of samples exhibiting trajectory errors of around 4 centimeters.

Figure 38 provides a visual representation of the trajectory errors observed in the experiment. Notably, the figure reveals that the areas with higher sample density tend to exhibit higher trajectory errors. This correlation suggests that the presence of more data samples in certain areas can introduce greater variability in the trajectory estimation. To address this issue and reduce the overall error, a data cleaning process can be implemented. By applying appropriate data cleaning techniques, such as outlier removal or noise reduction algorithms, the impact of data points with higher trajectory errors can be mitigated. This data cleaning process aims to enhance the accuracy and reliability of the trajectory estimation by minimizing the influence of erroneous or inconsistent measurements.

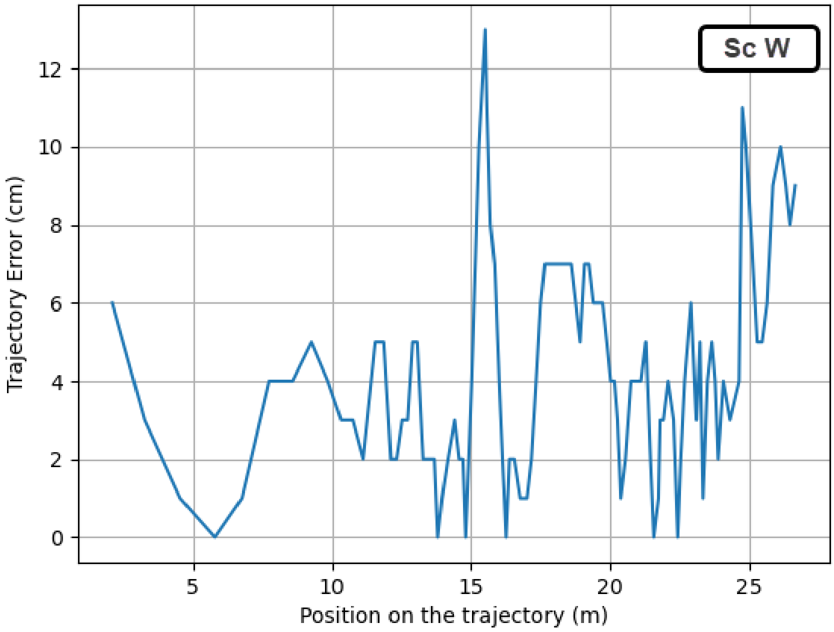

Figure 38: Trajectory Error for walking scenario

Cumulative distribution function of walking scenario indicates 95 percent likelihood is 9.95 centimeters which means 95 percents of data have trajectory error less than 9.95 centimeter and 90 precent likelihood is 7.9-centimeter Fig.39. According to the cumulative distribution function (CDF) analysis of the walking scenario (as shown in Figure 39), it can be observed that there is a 95 percent likelihood that the trajectory error is less than 9.95 centimeters. This indicates that 95 percent of the collected data in this scenario exhibit a trajectory error of 9.95 centimeters or lower.

Furthermore, the analysis reveals a 90 percent likelihood that the trajectory error is less than 7.9 centimeters. This means that 90 percent of the data points in the walking scenario demonstrate a trajectory error of 7.9 centimeters or less. By examining the CDF and interpreting the corresponding likelihood values, we can gain insights into the distribution and precision of the trajectory errors in the walking scenario. These findings allow researchers to assess the performance and reliability of the system, providing valuable information for further analysis and optimization.

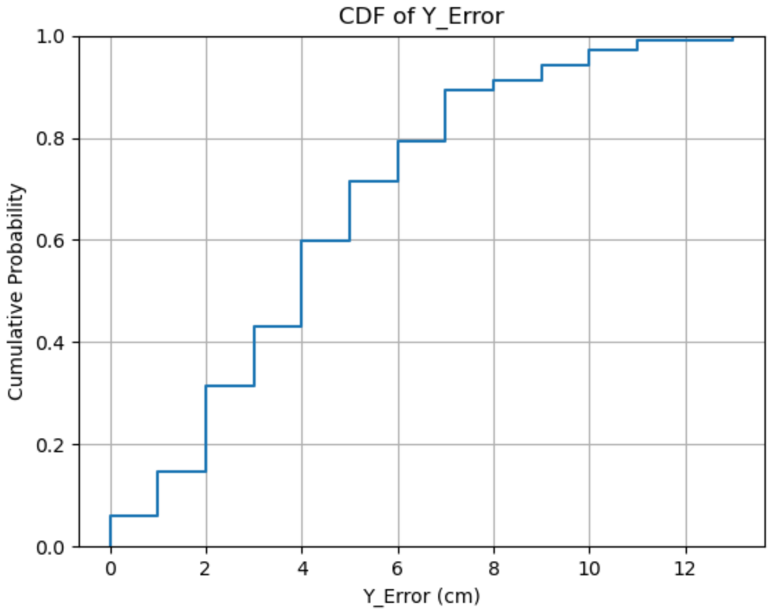

Figure 39: Cumulative distribution function of walking scenario

Second scenario running:

The second scenario entailed running along the specified line. Throughout the test, a total of 41 samples were collected, and the testing duration was 7.62 seconds, covering the full 28-meter path. In Figure 40, the data collected in this scenario is presented in a tabular format, accompanied by descriptive statistics such as the minimum, maximum, mean, and standard deviation. The results and statistics obtained from this scenario contribute to the overall assessment and analysis of the system's performance during running activities. By considering the minimum and maximum values, researchers can understand the range of measurements achieved. The mean value provides an estimate of the average position, while the standard deviation offers insights into the variability and precision of the measurements obtained during running.

	Time	X	Y	Z	TagQuality	Y_Error
count	41.000000	41.000000	41.000000	41.000000	41.000000	41.000000
mean	5.013902	15.320732	7.896341	0.607073	86.317073	14.073171
std	1.620703	7.028291	0.114908	0.158149	9.086911	6.258555
min	0.000000	1.360000	7.750000	0.170000	66.000000	1.000000
25%	4.010000	10.600000	7.820000	0.530000	79.000000	11.000000
50%	5.010000	15.560000	7.860000	0.620000	90.000000	15.000000
75%	6.120000	20.550000	7.940000	0.680000	94.000000	18.000000
max	7.620000	26.350000	8.200000	1.020000	99.000000	25.000000

Figure 40: Description of the data collection during running scenario.

Figure 41 provides a comprehensive visual representation of the collected data, showcasing the spatial arrangement of data samples, anchors, and the line path. The visualization enables an intuitive understanding of the dataset. Upon examining the figure, it can be observed that there are fewer variations in the density of data samples along the line path compared to the walking scenario. However, it is worth noting that there are areas where the tag quality is low. The presence of metal objects in the environment can have a significant impact on tag quality, thereby affecting the accuracy and reliability of the measurements. Objects with high conductivity, such as metal, can introduce challenges such as signal reflections, multipath interference, or signal attenuation. Additionally, the tag being attached to a person introduces another consideration. The human body can absorb signals, which can impact the tag quality and signal propagation. This absorption of signals by the body can further contribute to variations in the tag quality and affect the overall reliability of the measurements.

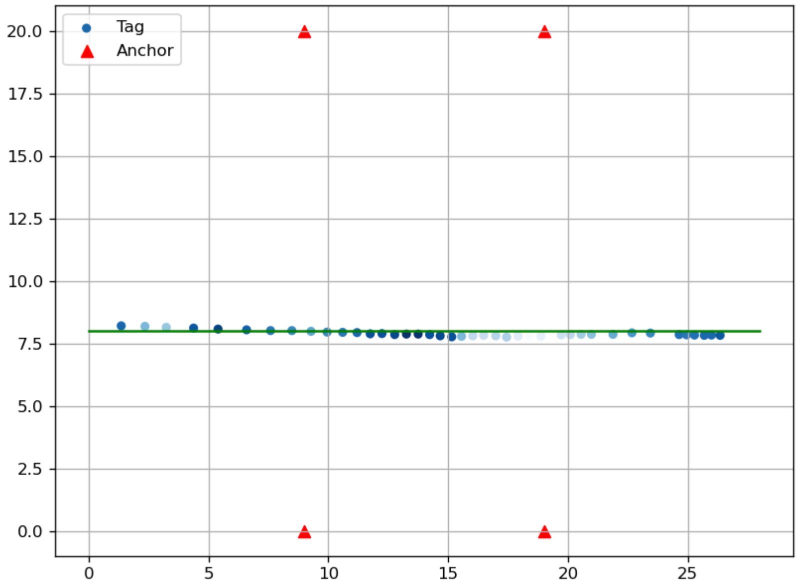

Figure 41: Visualization of second scenario

The trajectory error in this scenario was determined to be below 25 centimeters, with a mean error of 14 centimeters. Figure 42 visually displays the trajectory errors observed during the experiment. Upon analyzing the figure, it becomes evident that the trajectory error starts at around 20 centimeters and gradually decreases to approximately 1 centimeter. Following this decrease, the trajectory error then begins to fluctuate and subsequently increases towards the end of the experiment, reaching a value of 17 centimeters.

These variations in trajectory error can arise from various factors, such as environmental conditions, signal interference, or limitations of the tracking system or methodology employed. It is important to further investigate the specific causes of the fluctuations and increases in trajectory error to gain a comprehensive understanding of the underlying factors influencing the results.

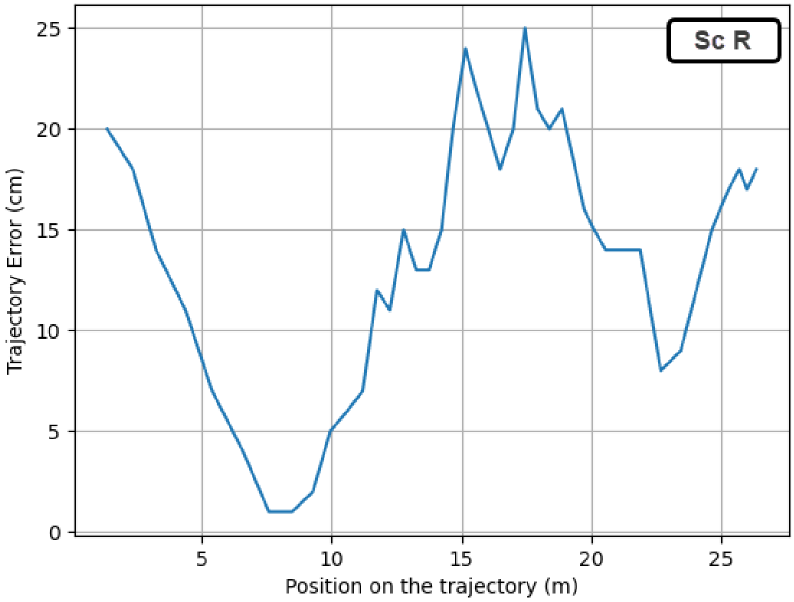

Figure 42: Trajectory Error for running scenario.

The cumulative distribution function (CDF) analysis of the running scenario, as illustrated in Figure 43, indicates a 95 percent likelihood that the trajectory error is less than 22 centimeters. This means that 95 percent of the collected data in the running scenario exhibit a trajectory error of 22 centimeters or lower. Additionally, there is a 90 percent likelihood that the trajectory error is less than 21 centimeters, indicating that 90 percent of the data points in the running scenario demonstrate a trajectory error of 21 centimeters or less.

However, it is important to note that, in comparison to the walking scenario, the data collected in the running scenario are deemed to be less reliable. This suggests that the trajectory errors observed in the running scenario may exhibit greater variability or inconsistency. Researchers should carefully analyze the trajectory errors in the running scenario to identify potential factors that contribute to the decreased reliability of the data.

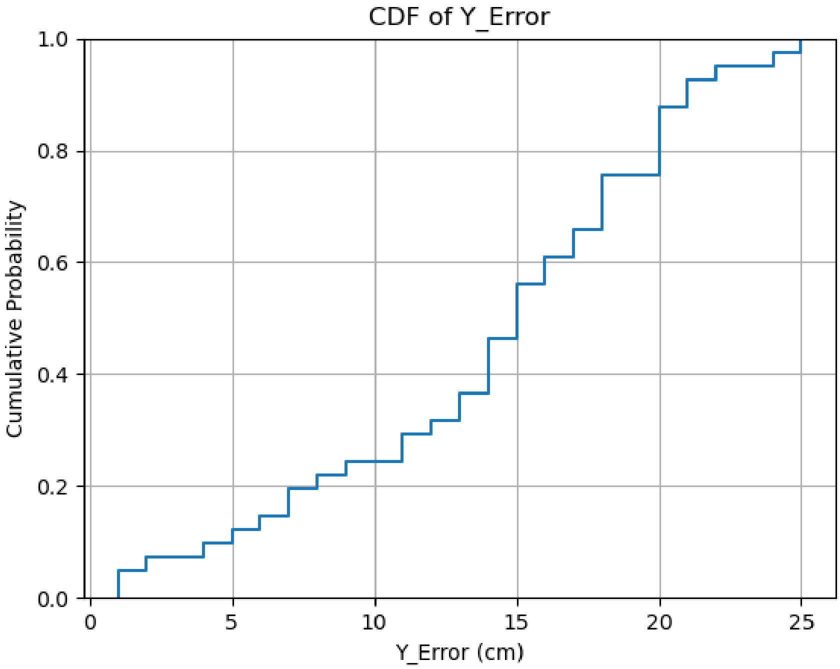

Figure 43: Cumulative distribution function of running scenario.

Third scenario running faster than second scenario:

In the third scenario, participants were instructed to run at a fast speed along the designated line. A total of 38 samples were collected during the test, which had a duration of 6.61 seconds, covering the entire 28-meter path. Figure 44 presents the data collected in this scenario in a data-frame format, along with descriptive statistics including the minimum, maximum, mean, and standard deviation. The mean value, which is approximately 85 percent for tag quality, represents the average performance of the tags in accurately estimating the position. It is worth noting that the tag quality of the two previous scenarios is also approximately 85 percent. This consistency in tag quality across the scenarios suggests that the system maintained a similar level of performance throughout different running speeds.

	Time	X	Y	Z	TagQuality	Y_Error
count	38.000000	38.000000	38.000000	38.000000	38.000000	38.000000
mean	5.163421	15.855789	7.922368	0.711053	85.131579	10.289474
std	1.691723	7.304849	0.080687	0.211798	8.621692	4.273791
min	0.000000	1.500000	7.800000	0.300000	68.000000	0.000000
25%	4.225000	11.100000	7.872500	0.630000	78.250000	8.000000
50%	5.310000	16.470000	7.910000	0.695000	86.000000	10.000000
75%	6.385000	21.580000	7.930000	0.765000	91.750000	12.750000
max	7.610000	26.480000	8.120000	1.560000	99.000000	20.000000

Figure 44: Description of the data collection during run at fast speed scenario

Similar to previous visualizations, Figure 45 offers a visual representation of the collected data, providing insight into the spatial arrangement of data samples, anchors, and the line path. By analyzing the figure, it becomes evident that there are variations in the density of data samples along the line path. Some areas exhibit higher sample density, while others appear sparser.

Moreover, it is important to acknowledge that areas with low tag quality are present within the depicted visualization. As previously mentioned, the tag quality can be affected by various factors such as the presence of metal objects in the environment or the absorption effects of the human body. Understanding the variations in sample density and the presence of areas with low tag quality is essential for researchers. These observations provide valuable information about the spatial distribution of the collected data and highlight potential limitations or challenges that may affect the overall reliability and precision of the measurements.

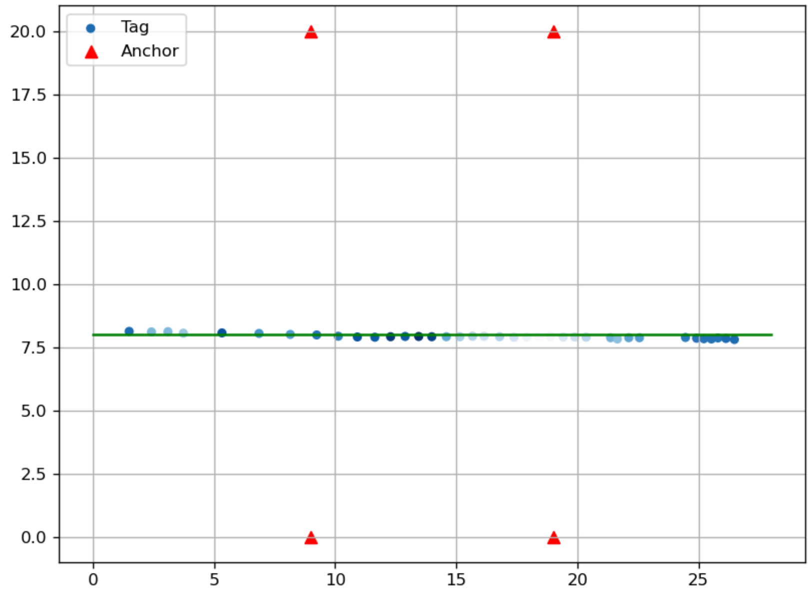

Figure 45: Visualization of third scenario

The trajectory error in this particular scenario was found to be below 20 centimeters, with a mean error of 10.3 centimeters. Figure 46 provides a visual representation of the observed trajectory errors during the experiment. Upon examining the figure, it is evident that the trajectory error initially starts at around 12.5 centimeters and gradually decreases towards approximately 0 centimeters. This decrease suggests an improvement in the accuracy of the estimated trajectory. However, following this decrease, the trajectory error begins to fluctuate and subsequently increases towards the end of the experiment, reaching a value of 20 centimeters. These variations in trajectory error can be attributed to various factors that may influence the accuracy and precision of the measurements. Environmental conditions, such as the presence of obstacles or signal-blocking objects, can affect the propagation of signals and introduce deviations in the estimated trajectory. Signal interference from other wireless devices or sources can also impact the accuracy of the measurements.

Additionally, limitations in the tracking system or methodology employed can contribute to fluctuations and increases in trajectory error. Factors such as the positioning accuracy of the anchors, the quality of the received signals, or the algorithms used for trajectory estimation can influence the overall accuracy and consistency of the results. To gain a comprehensive understanding of the underlying factors influencing the observed trajectory errors, further investigation is necessary. Researchers can analyze the specific causes of the fluctuations and increases in trajectory error, consider the environmental conditions and potential sources of interference, and assess the limitations of the tracking system or methodology. This investigation can help identify areas for improvement and guide the refinement of the measurement system or experimental setup.

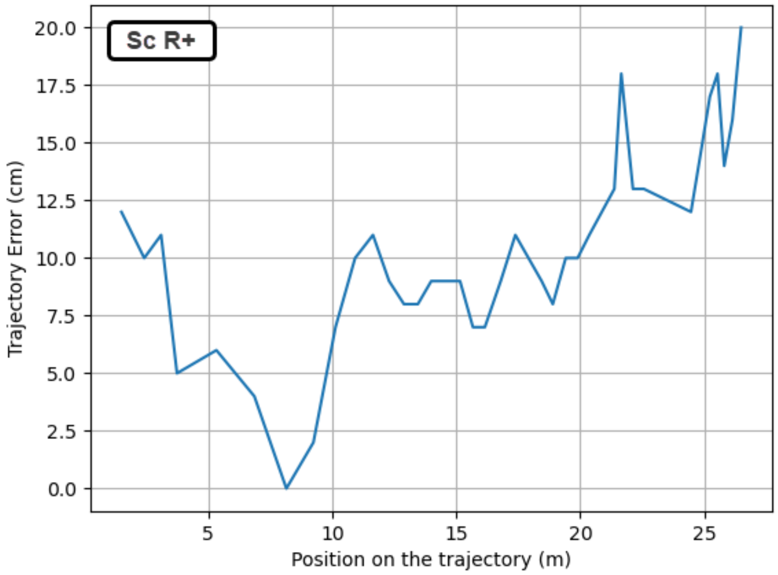

Figure 46: Trajectory Error for running scenario.

Based on the cumulative distribution function (CDF) analysis of the running faster scenario, as depicted in Figure 47, it is observed that there is a 95 percent likelihood that the trajectory error is less than 18 centimeters. By examining the CDF and interpreting the associated likelihood values, researchers gain valuable insights into the distribution and precision of the trajectory errors in the running faster scenario. These likelihood values provide quantitative measures of the performance and accuracy of the system when tracking fast-paced movements.

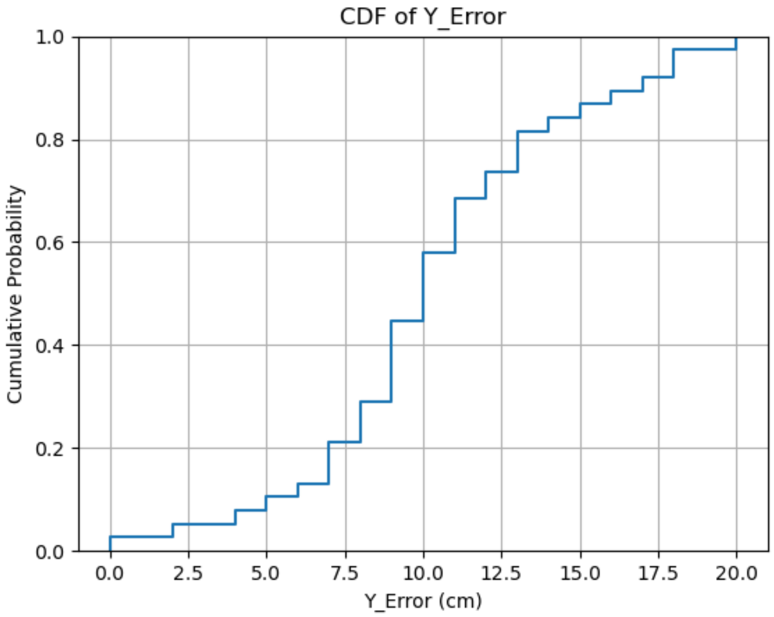

Figure 47: Cumulative distribution function of running faster scenario.

Fourth scenario The Sprint-Walk-Run Combination Scenario:

In the final scenario, participants embark on an engaging journey of diverse movements. The scenario commences with an acceleration phase, where participants gradually gain speed over the first 12 meters of the designated path. Subsequently, participants transition into a deceleration phase, gradually reducing their speed over the next 8 meters. Afterward, participants seamlessly transition into a steady walking pace, maintaining this rhythm for the subsequent 4 meters. Finally, the scenario concludes with participants instructed to run for the last 4 meters, culminating the dynamic combination.

Throughout the test, a total of 66 samples were collected, capturing the intricacies of each movement. The test duration encompassed 8.11 seconds, encompassing the entirety of the 28-meter path. Figure 48 showcases the data collected in this scenario, presented in a data-frame format. The descriptive statistics accompanying the data include essential metrics such as the minimum, maximum, mean, and standard deviation. Notably, the mean value for tag quality is approximately 85 percent.

	Time	X	Y	Z	TagQuality	Y_Error
count	66.000000	66.000000	66.000000	66.000000	66.000000	66.000000
mean	4.326212	18.648485	7.963939	0.702273	84.666667	4.181818
std	2.233321	6.360729	0.044024	0.438405	9.264213	3.850711
min	0.000000	2.110000	7.800000	0.190000	68.000000	0.000000
25%	2.625000	15.465000	7.950000	0.467500	76.000000	1.250000
50%	4.255000	19.600000	7.970000	0.635000	87.500000	3.000000
75%	6.085000	22.657500	7.990000	0.777500	92.750000	6.000000
max	8.110000	27.690000	8.080000	3.000000	99.000000	20.000000

Figure 48: Description of the data during Sprint-Walk-Run Combination Scenario

Similar to previous visualizations, Fig.49 offers a visual representation of the data, providing insight of data samples, anchors, and the the line path. By analyzing the figure, it becomes evident that samples in the beginning test are more sparse, and the reason can be player accelarate and increase his speed so there would be less time to collect data.

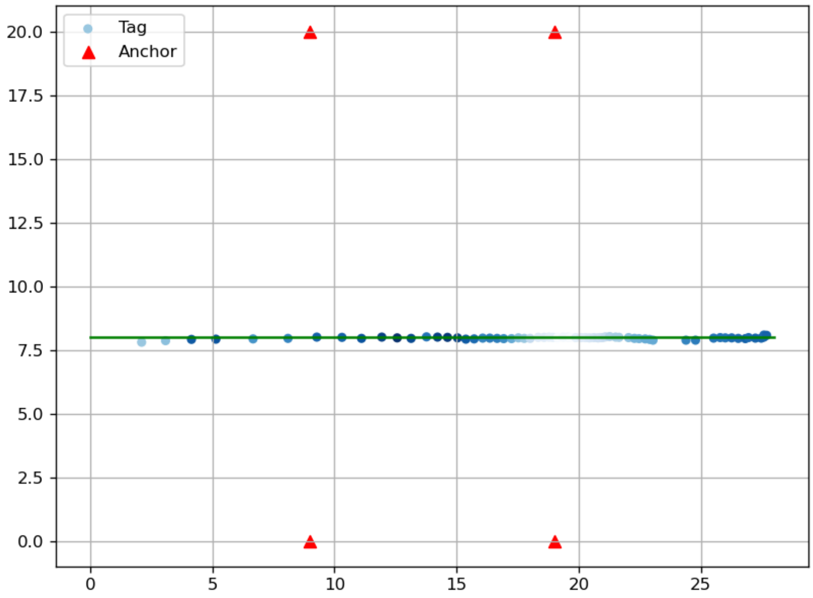

Figure 49: Visualization of fourth scenario

The trajectory error in this particular scenario was found to be below 20 centimeters, with a mean error of 4.11 centimeters. Figure 50 provides a visual representation of the observed trajectory errors during the experiment. Upon examining the figure, it is evident that the trajectory error initially starts at around 20 centimeters and gradually decreases towards approximately 0 centimeters. This decrease suggests an improvement in the accuracy of the estimated trajectory. However, following this decrease, the trajectory error begins to fluctuate and subsequently increases towards the end of the experiment, reaching a maximum value of 12 centimeters.

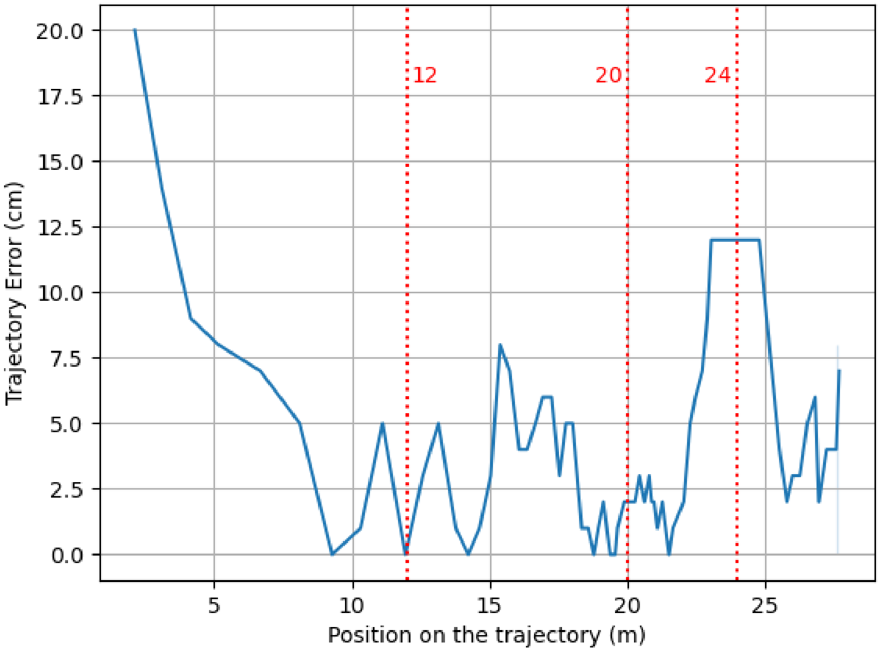

Figure 50: Trajectory Error for Sprint-Walk-Run Combination Scenario.

Based on the cumulative distribution function (CDF) analysis of the sprint-walk-run scenario, as depicted in Figure 51, it is observed that there is a 95 percent likelihood that the trajectory error is less than 12 centimeters. By examining the CDF and interpreting the associated likelihood values, researchers gain valuable insights into the distribution and precision of the trajectory errors in the sprint-walk-run scenario. These likelihood values provide quantitative measures of the performance and accuracy of the system when tracking fast-paced movements.

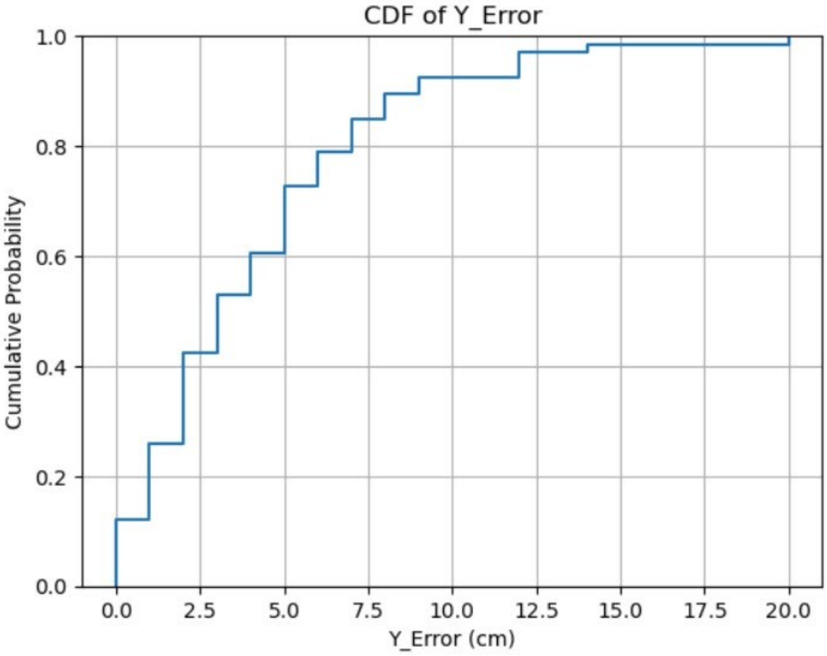

Figure 51: Cumulative distribution function of sprint-walk-run scenario.

CHAPTER 5: Conclusions:

- To comprehensively compare and evaluate all scenarios, we have the trajectories into a single figure, namely Figure 52. This visual representation allows for an analysis of the system's performance across different scenarios. Upon examining Figure 52, it becomes apparent that the trajectories closely align with the designated path for all scenarios. The system captures and follows the intended movements, highlighting its ability to accurately estimate positions throughout the diverse locomotion scenarios.

- It is worth noting that the tag emitting rate for this experiment is set at 10Hz, capturing data at a relatively high frequency. However, as the speed of the movement increases, the number of valid data positions decreases. This phenomenon occurs due to the limitations of the tracking system in capturing precise measurements during high-speed motions. Nonetheless, even with this limitation, the system still manages to provide meaningful and reliable trajectory estimations.

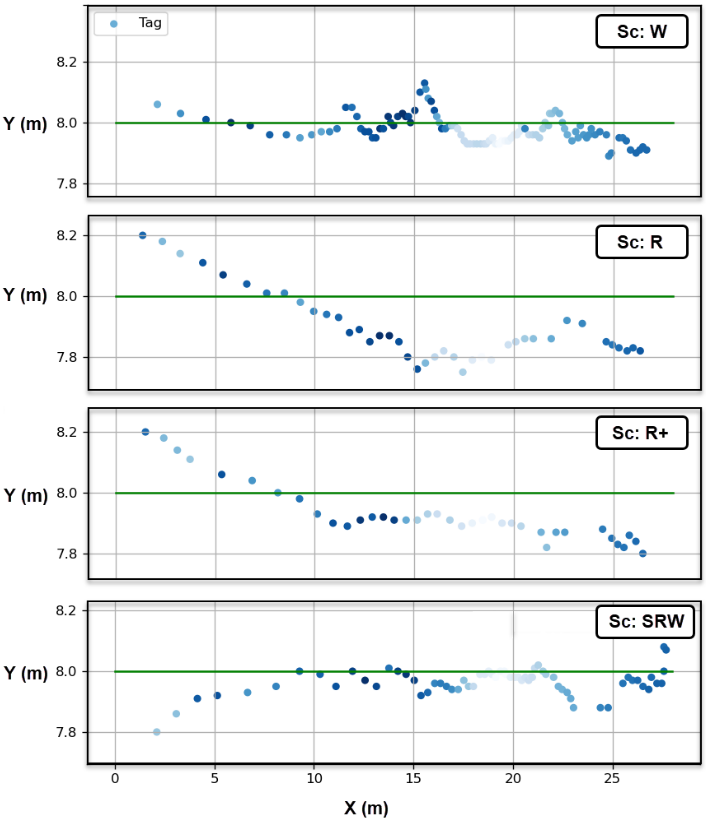

Figure 52: Vizualisation of the estimateed position for the 4 scenarios

- By analyzing the figure, it is apparent that the maximum error observed in all scenarios is approximately 20cm. The ability to estimate positions within a range of 15-20cm fulfills the requirements of the sports domain and provides sufficient precision for tracking and analyzing athlete movements [65].

Figure 53 presents the cumulative distribution function (CDF) of all the scenarios, offering valuable insights into the performance of the system across different motion patterns and speeds. By analyzing the graphs, several observations can be made, providing a basis for meaningful conclusions.

- The CDF graphs indicate that the walking and sprint-walk-run scenarios exhibit better results compared to the running and running fast scenarios. This observation suggests that the system's accuracy and precision in estimating positions are higher during walking and the dynamic combination of sprinting, walking, and running. These scenarios likely involve more consistent and predictable movements, allowing for more reliable trajectory estimations.

- It can be inferred that the change in motion patterns of the player, such as transitioning from walking to running, does not significantly impact the overall results. This finding suggests that the system is robust and capable of effectively adapting to different motion patterns, providing consistent and accurate position estimations across various locomotion scenarios.

- A noteworthy observation is that increasing the speed, as seen in the running and running fast scenarios, may lead to higher errors in the position estimations. This can be attributed to the shorter duration of the faster movements, resulting in a decreased amount of data and potentially higher variability in the measurements. The limited data availability at higher speeds can contribute to less precise position estimations and, consequently, a higher likelihood of errors.

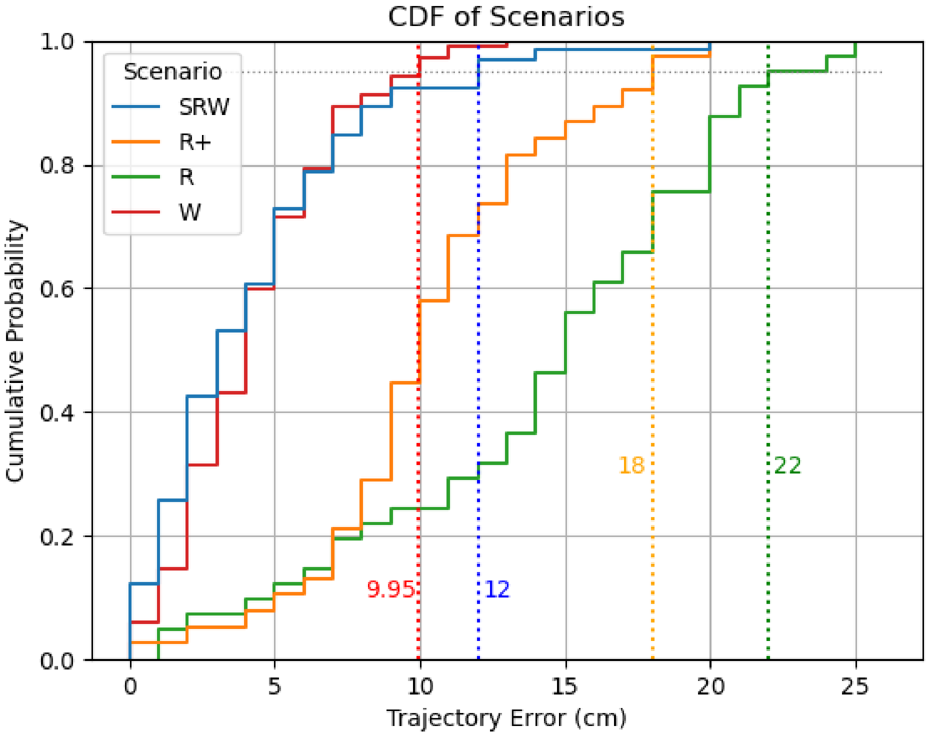

Figure 53: the cumulative distribution function (CDF) of all the scenarios

Bibliography

[1] F. Zafari, A. Gkelias, and K. Leung, “A Survey of Indoor Localization Systems and Technologies.” arXiv, Jan. 16, 2019. Accessed: May 03, 2023. [Online]. Available: http://arxiv.org/abs/1709.01015

[2] X. Chi, G. Wu, J. Xu, J. Liu, and Q. Lu, “Review on Ultra Wide Band Indoor Localization,” 2020.

[3] Salvatore Dello Iacono, Vincenzo Paciello, and Paolo Sommella, “Distance Measurement Characterization for Ultra Wide Band Indoor Localization Systems,” *Int. Instrum. Meas. Technol. Conf.*, May 2022, doi: 10.1109/i2mtc48687.2022.9806537.

[4] X. Chi, G. Wu, J. Liu, J. Xu, and Q. Lu, “Review on Ultra Wide Band Indoor Localization,” vol. 2, no. 2, pp. 99–110, 2020, doi: 10.35806/ijoced.v2i2.118.

[5] S. Lingesh and G. Shobha, “Localization of Ultra Wide-Band Enabled Devices,” *2022 IEEE 3rd Glob. Conf. Adv. Technol. GCAT*, 2022, doi: 10.1109/gcat55367.2022.9971863.

[6] H. A. Obeidat, W. Shuaieb, O. Obeidat, and R. A. Abd-Alhameed, “A Review of Indoor Localization Techniques and Wireless Technologies,” *Wirel. Pers. Commun.*, vol. 119, no. 1, pp. 289–327, 2021, doi: 10.1007/s11277-021-08209-5.

[7] G. Raj, Vishal P Roy, and Dhanesh M.S, “Indoor Localization based on Ultra Wide Band using Deca-Wave,” 2020.

[8] M. A. Al-Ammar *et al.*, “Comparative Survey of Indoor Positioning Technologies, Techniques, and Algorithms,” in *2014 International Conference on Cyberworlds*, Santander, Cantabria, Spain: IEEE, Oct. 2014, pp. 245–252. doi: 10.1109/CW.2014.41.

[9] A. Waqar, I. Ahmad, D. Habibi, and Q. V. Phung, “Analysis of GPS and UWB positioning system for athlete tracking,” *Meas. Sens.*, vol. 14, p. 100036, Apr. 2021, doi: 10.1016/j.measen.2020.100036.

[10] A. Conti, D. Dardari, and M. Z. Win, “Experimental results on cooperative UWB based positioning systems,” in *2008 IEEE International Conference on Ultra-Wideband*, Hannover: IEEE, Sep. 2008, pp. 191–195. doi: 10.1109/ICUWB.2008.4653316.

[11] P. Cotera, M. Velazquez, D. Cruz, L. Medina, and M. Bandala, “Indoor Robot Positioning Using an Enhanced Trilateration Algorithm,” *Int. J. Adv. Robot. Syst.*, vol. 13, no. 3, p. 110, May 2016, doi: 10.5772/63246.

[12] A. Aguilar-Garcia, S. Fortes, R. Barco, and E. Colin, “Enhancing localization accuracy with multi-antenna UHF RFID fingerprinting,” *Int. Conf. Indoor Position. Indoor Navig.*, pp. 1–9, Oct. 2015, doi: 10.1109/ipin.2015.7346938.

[13] Y. Wang, C. Xiu, X. Zhang, D. Yang, and Dongkai Yang, “WiFi Indoor Localization with CSI Fingerprinting-Based Random Forest.,” *Sensors*, vol. 18, no. 9, p. 2869, Aug. 2018, doi: 10.3390/s18092869.

[14] J. Jeon, Y. Kong, Y. Nam, and K. Yim, “An Indoor Positioning System Using Bluetooth RSSI with an Accelerometer and a Barometer on a Smartphone,” *Broadband Wirel. Comput. Commun. Appl.*, pp. 528–531, Nov. 2015, doi: 10.1109/bwcca.2015.142.

[15] B. Krishnaveni, K. Reddy, and P. Reddy, “Wireless Indoor Positioning Techniques Based on Ultra Wideband (UWB) Technology,” 2019.

[16] A. Aguilar-Garcia, S. Fortes, E. Colin, and R. Barco, “Enhancing RFID indoor localization with cellular technologies,” *Eurasip J. Wirel. Commun. Netw.*, vol. 2015, no. 1, p. 219, Sep. 2015, doi: 10.1186/s13638-015-0444-9.

[17] Z. Liu, R. Chen, F. Ye, G. Guo, and L. Huang, “a Low-Delay and Robust Solution for Rapid Movement Detection Using Uwb,” *ISPRS - Int. Arch. Photogramm. Remote Sens. Spat. Inf. Sci.*, pp. 377–382, Aug. 2020, doi: 10.5194/isprs-archives-xliii-b1-2020-377-2020.

[18] V. Gharat, E. Colin, G. Baudoin, and D. Richard, “Indoor performance analysis of LF-RFID based positioning system: Comparison with UHF-RFID and UWB,” *Int. Conf. Indoor Position. Indoor Navig.*, pp. 1–8, Sep. 2017, doi: 10.1109/ipin.2017.8115901.

[19] Mahmoud Elsanhoury *et al.*, “Precision Positioning for Smart Logistics using Ultra-Wideband Technology-Based Indoor Navigation: a Review,” *IEEE Access*, pp. 1–1, Jan. 2022, doi: 10.1109/access.2022.3169267.

[20] M. Ridolfi *et al.*, “Experimental Evaluation of UWB Indoor Positioning for Sport Postures.,” *Sensors*, vol. 18, no. 1, p. 168, Jan. 2018, doi: 10.3390/s18010168.

[21] A. J. Coutts and R. Duffield, “Validity and reliability of GPS devices for measuring movement demands of team sports,” *J. Sci. Med. Sport*, vol. 13, no. 1, pp. 133–135, Jan. 2010, doi: 10.1016/j.jsams.2008.09.015.

[22] A. Alarifi *et al.*, “Ultra Wideband Indoor Positioning Technologies: Analysis and Recent Advances.,” *Sensors*, vol. 16, no. 5, p. 707, May 2016, doi: 10.3390/s16050707.

[23] Aoran Xiao *et al.*, “An Indoor Positioning System Based on Static Objects in Large Indoor Scenes by Using Smartphone Cameras.,” *Sensors*, vol. 18, no. 7, p. 2229, Jul. 2018, doi: 10.3390/s18072229.

[24] R. Mautz and R. Mautz, “The challenges of indoor environments and specification on some alternative positioning systems,” *Workshop Position. Navig. Commun.*, pp. 29–36, Mar. 2009, doi: 10.1109/wpnc.2009.4907800.

[25] V. De Silva *et al.*, “Player Tracking Data Analytics as a Tool for Physical Performance Management in Football: A Case Study from Chelsea Football Club Academy.,” *Sports*, vol. 6, no. 4, p. 130, Oct. 2018, doi: 10.3390/sports6040130.

[26] T. Dima, “The Business Model of European Football Club Competitions,” *Procedia Econ. Finance*, vol. 23, pp. 1245–1252, Jan. 2015, doi: 10.1016/s2212-5671(15)00562-6.

[27] Hui Liu, H. Liu, H. Darabi, P. Banerjee, and J. Liu, “Survey of Wireless Indoor Positioning Techniques and Systems,” *IEEE Trans. Syst. Man Cybern. Part C Appl. Rev.*, vol. 37, no. 6, pp. 1067–1080, Nov. 2007, doi: 10.1109/tsmcc.2007.905750.

[28] S. Ilarri, E. Mena, A. Illarramendi, and G. Marcos, “A location-aware system for monitoring sport events,” *Adv. Mob. Multimed.*, pp. 297–304, Nov. 2010, doi: 10.1145/1971519.1971569.

[29] R. Leser, A. Baca, and G. Ogris, “Local positioning systems in (game) sports.,” *Sensors*, vol. 11, no. 10, pp. 9778–9797, Oct. 2011, doi: 10.3390/s111009778.

[30] S. Barris and C. Button, “A Review of Vision-Based Motion Analysis in Sport,” *Sports Med.*, vol. 38, no. 12, pp. 1025–1043, Jan. 2008, doi: 10.2165/00007256-200838120-00006.

[31] G. Giblin, Georgia Giblin, E. Tor, Elaine Tor, Elaine Tor, and L. Parrington, “The impact of technology on elite sports performance,” *Sensoria J. Mind Brain Cult.*, vol. 12, no. 2, Nov. 2016, doi: 10.7790/sa.v12i2.436.

[32] T. Mirzoev, “Low Rate Wireless Personal Area Networks (LR-WPAN 802.15.4 standard).,” *ArXiv Netw. Internet Archit.*, Apr. 2014.

[33] Jeonghyeon Cheon, J. Cheon, H.-S. Hwang, Hyunsu Hwang, D. Kim, and Y. Jung, “IEEE 802.15.4 ZigBee-Based Time-of-Arrival Estimation for Wireless Sensor Networks,” *Sensors*, vol. 16, no. 2, pp. 203–203, Feb. 2016, doi: 10.3390/s16020203.

[34] L. Mucchi *et al.*, “A Flexible Wireless Sensor Network Based on Ultra-Wide Band Technology for Ground Instability Monitoring.,” *Sensors*, vol. 18, no. 9, p. 2948, Sep. 2018, doi: 10.20944/preprints201807.0380.v1.

[35] C. E. Galván-Tejada, J.-P. García-Vázquez, and R. F. Brena, “Magnetic Field Feature Extraction and Selection for Indoor Location Estimation,” *Sensors*, vol. 14, no. 6, pp. 11001–11015, Jun. 2014, doi: 10.3390/s140611001.

[36] S. Pala and D. G. Kurup, “A Leading Edge Detection Algorithm for UWB Based Indoor Positioning Systems,” *Lect. Notes Inst. Comput. Sci. Soc. Inform. Telecommun. Eng.*, pp. 45–55, Mar. 2021, doi: 10.1007/978-3-030-79276-3_4.

[37] Y. Gao, O. Postolache, Y. Yang, and B. Yang, “UWB System and Algorithms for Indoor Positioning,” *2021 Telecoms Conf. ConfTELE*, Feb. 2021, doi: 10.1109/conftele50222.2021.9435577.

[38] A. Safaei and I. Sharf, “Velocity estimation for UAVs using ultra wide-band system,” *Int. Conf. Unmanned Aircr. Syst.*, Jun. 2021, doi: 10.1109/icuas51884.2021.9476831.

[39] A. A. Hadipranoto, “Design and Construction of an Indoor Positioning System Based on the DWM1000 Ultra-Wideband (UWB) Module = Perancangan dan pembuatan sistem pelacak posisi berbasis modul ultra-wideband (uWB) DWM1000,” Feb. 2020.

[40] P. Grasso, M. S. Innocente, Jun Jet Tai, O. C. L. Haas, and A. M. Dizqah, “Analysis and Accuracy Improvement of UWB-TDoA-Based Indoor Positioning System,” *Sensors*, vol. 22, no. 23, pp. 9136–9136, Nov. 2022, doi: 10.3390/s22239136.

[41] B. Li, Z. Hao, Zhanjun Hao, X. Dang, and Xiaochao Dang, “An indoor location algorithm based on Kalman filter fusion of ultra-wide band and inertial measurement unit,” *AIP Adv.*, vol. 9, no. 8, p. 085210, Aug. 2019, doi: 10.1063/1.5117341.

[42] Daizhuang Bai, Tongyue Gao, Weiping Guo, Xiaobing Wang, and Jinwang Li, “Research on pedestrian indoor positioning technology integrating UWB and PDR,” *Conf.*, Nov. 2022, doi: 10.1117/12.2652547.

[43] P. Schwarzbach, R. Weber, and O. Michler, “Statistical Evaluation and Synthetic Generation of Ultra-Wideband Distance Measurements for Indoor Positioning Systems,” *IEEE Sens. J.*, pp. 1–1, Jan. 2021, doi: 10.1109/jsen.2021.3121627.

[44] Z. Liao, Z. Zheng, and Y. Li, “IMPLEMENTATION AND IMPROVEMENT OF INDOOR WEARABLE UWB/INS INTEGRATION POSITIONING METHOD,” *Int. Arch. Photogramm. Remote Sens. Spat. Inf. Sci.*, vol. XLVI-3/W1-2022, pp. 111–117, Apr. 2022, doi: 10.5194/isprs-archives-xlvi-3-w1-2022-111-2022.

[45] A. Albaidhani and A. Alsudani, “Anchor selection by geometric dilution of precision for an indoor positioning system using ultra-wide band technology,” *IET Wirel. Sens. Syst.*, vol. 11, no. 1, pp. 22–31, 2020, doi: 10.1049/wss2.12006.

[46] P. Dabove, V. Di Pietra, M. Piras, Marco Piras, A. A. Jabbar, and S. A. Kazim, “Indoor positioning using Ultra-wide band (UWB) technologies: Positioning accuracies and sensors’ performances,” *2018 IEEEION Position Locat. Navig. Symp. PLANS*, pp. 175–184, Apr. 2018, doi: 10.1109/plans.2018.8373379.

[47] Chenming Liu, “Ultra Wide Band Technology and Indoor Precise Positioning,” *SHS Web Conf.*, vol. 144, pp. 02002–02002, Jan. 2022, doi: 10.1051/shsconf/202214402002.

[48] Sixto Campaña Bastidas, Macarena Espinilla, and Javier Medina Quero, “Review of Ultra Wide Band (UWB) for Indoor Positioning with application to the elderly,” *Hawaii Int. Conf. Syst. Sci.*, Jan. 2022, doi: 10.24251/hicss.2022.269.

[49] Pengtao Wu, “Comparison between the Ultra-wide Band based indoor positioning technology and other technologies,” *J. Phys.*, vol. 2187, no. 1, pp. 012010–012010, Feb. 2022, doi: 10.1088/1742-6596/2187/1/012010.

[50] Slawomir Romaniuk, Adam Wolniakowski, Adam Pawlowski, and Cezary Kownacki, “Adaptation of Ultra Wide Band positioning system for Adaptive Monte Carlo Localization,” *Int. Conf. Methods Models Autom. Robot.*, Aug. 2022, doi: 10.1109/mmar55195.2022.9874314.

[51] A. Jiménez and F. Seco, “Finding objects using UWB or BLE localization technology: A museum-like use case,” *Int. Conf. Indoor Position. Indoor Navig.*, pp. 1–8, Sep. 2017, doi: 10.1109/ipin.2017.8115865.

[52] Jun Li, “Design of an Ultra-Wide Band based Indoor Positioning System DESIGN OF AN ULTRA-WIDE BAND BASED INDOOR POSITIONING SYSTEM,” 2018.

[53] M. Elsanhoury *et al.*, “Precision Positioning for Smart Logistics Using Ultra-Wideband Technology-Based Indoor Navigation: A Review,” *IEEE Access*, vol. 10, pp. 44413–44445, 2022, doi: 10.1109/ACCESS.2022.3169267.

[54] S. Subedi and J.-Y. Pyun, “A Survey of Smartphone-Based Indoor Positioning System Using RF-Based Wireless Technologies,” *Sensors*, vol. 20, no. 24, p. 7230, Dec. 2020, doi: 10.3390/s20247230.

[55] K. Wisiak, M. Jakić, and P. Hartlieb, “Application of Ultra-Wide Band Sensors in Mining,” *Sensors*, vol. 23, no. 1, p. 300, Dec. 2022, doi: 10.3390/s23010300.

[56] Y. Zhao, J. Zou, J. Guo, G. Huang, and L. Cai, “A Novel Ultra-Wideband Double Difference Indoor Positioning Method with Additional Baseline Constraint,” *ISPRS Int. J. Geo-Inf.*, vol. 10, no. 10, p. 634, Sep. 2021, doi: 10.3390/ijgi10100634.

[57] R. S. Kulikov, “Integrated UWB/IMU system for high rate indoor navigation with cm-level accuracy,” in *2018 Moscow Workshop on Electronic and Networking Technologies (MWENT)*, Moscow: IEEE, Mar. 2018, pp. 1–4. doi: 10.1109/MWENT.2018.8337235.

[58] P. T. Lin, C.-A. Liao, and S.-H. Liang, “Probabilistic Indoor Positioning and Navigation (PIPN) of Autonomous Ground Vehicle (AGV) Based on Wireless Measurements,” *IEEE Access*, vol. 9, pp. 25200–25207, 2021, doi: 10.1109/ACCESS.2021.3057415.

[59] B. Feng and Q. Ye, “Operations management of smart logistics: A literature review and future research,” *Front. Eng. Manag.*, vol. 8, no. 3, pp. 344–355, Sep. 2021, doi: 10.1007/s42524-021-0156-2.

[60] “MDEK1001 Kit User Manual Module Development & Evaluation Kit for the DWM1001.”

[61] Y. Giannouris, “History of Water Polo – The Beginning.” https://learning.fina.org/history-of-water-polo/

[62] “Water polo-rules.” https://www.worldaquatics.com/water-polo/rules

[63] “Sciences 2024.” https://sciences2024.polytechnique.fr

[64] “Qorvo MDEK1001, Ultral-Wideband (UWB) Transceiver Kit.” https://www.qorvo.com/products/p/MDEK1001

[65] R. M. Gonzalez, L. Arcos, P. Ortega, and M. Nakamura, “The use of technology and sampling frequency to measure variables of tactical positioning in team sports: A systematic review,” *Res. Sports Med.*, no. 28(2), pp. 279–292, 2020.

[66] K. Suresh *et al.*, “Simultaneous Detection of Multiple Surface Acoustic Wave Sensor Tags for Water Quality Monitoring Utilizing Cellular Code-Reuse Approach,” *IEEE Internet Things J.*, vol. 9, no. 16, pp. 14385–14399, Aug. 2022, doi: 10.1109/JIOT.2021.3082141.

[67] P. Dabove, V. Di Pietra, M. Piras, A. A. Jabbar, and S. A. Kazim, “Indoor positioning using Ultra-wide band (UWB) technologies: Positioning accuracies and sensors’

performances," in *2018 IEEE/ION Position, Location and Navigation Symposium (PLANS)*, Monterey, CA: IEEE, Apr. 2018, pp. 175–184. doi: 10.1109/PLANS.2018.8373379.

[68] F. Sabath, E. L. Mokole, and S. N. Samaddar, "Definition and Classification of Ultra-Wideband Signals and Devices," no. 313, 2005.

[69] J.-S. Lee, Y.-W. Su, and C.-C. Shen, "A Comparative Study of Wireless Protocols: Bluetooth, UWB, ZigBee, and Wi-Fi," in *IECON 2007 - 33rd Annual Conference of the IEEE Industrial Electronics Society*, Taipei, Taiwan: IEEE, 2007, pp. 46–51. doi: 10.1109/IECON.2007.4460126.

[70] A. Yassin *et al.*, "Recent Advances in Indoor Localization: A Survey on Theoretical Approaches and Applications," *IEEE Commun. Surv. Tutor.*, vol. 19, no. 2, pp. 1327–1346, 2017, doi: 10.1109/COMST.2016.2632427.

[71] A. Rácz-Szabó, T. Ruppert, L. Bántay, A. Löcklin, L. Jakab, and J. Abonyi, "Real-Time Locating System in Production Management," *Sensors*, vol. 20, no. 23, p. 6766, Nov. 2020, doi: 10.3390/s20236766.

[72] M. Ridolfi *et al.*, "Experimental Evaluation of UWB Indoor Positioning for Sport Postures," *Sensors*, vol. 18, no. 2, p. 168, Jan. 2018, doi: 10.3390/s18010168.

[73] K. Khurshid and I. A. Khokhar, "Comparison survey of 4G competitors (OFDMA, MC CDMA, UWB, IDMA)," in *2013 International Conference on Aerospace Science & Engineering (ICASE)*, Islamabad, Pakistan: IEEE, Aug. 2013, pp. 1–7. doi: 10.1109/ICASE.2013.6785555.

CANDIDATE CURRICULUM VITAE & REFERENCES

https://www.linkedin.com/in/farshadshamlu/